國立台灣大學臨床醫學研究所

博士論文

Graduate Institute of Clinical Medicine

College of Medicine

National Taiwan University

Doctoral Dissertation

S14 在內分泌及代謝疾病中的角色：臨床與基礎研究

The roles of S14 in endocrine and metabolic disorders: clinical and basic studies

陳彥婷

Yen-Ting Chen

指導教授: 楊偉勛教授、黃天祥教授

Professor Wei-Shiung Yang, Professor Tien-Shang Huang

中華民國 108 年 6 月

June, 2019

doi:10.6342/NTU201901578

國立臺灣大學博士學位論文
口試委員會審定書

S14 在內分泌及代謝疾病中的角色：臨床與基礎研究

The roles of S14 in endocrine and metabolic disorders: clinical and basic studies

本論文係陳彥婷君（學號 D96448007）在國立臺灣大學臨床醫學研究所完成之博士學位論文，於民國 108 年 6 月 17 日承下列考試委員審查通過及口試及格，特此證明

口試委員：

黃天祥	林偉勛（簽名）
（指導教授）	
蔣曜聲	阮雪真
陳泳隆	

系主任、所長 林偉勛（簽名）

誌謝

人的一生總會遇到一些關卡以及許多的選擇題，而每個人的人生就只有那麼一次，無法走回頭路，永遠沒有人會知道如果當初做了另一個選擇，人生是否會有所不同……

博士班求學的旅程有歡笑也有悲苦，陰天、雨天、颱風天、晴天、星空與彩虹，生命科學如此地奧秘，人能掌控的事物其實並不多，為了追尋夢想、完成當初入學的心願：在基礎研究發展技術或是理論，在未來幫助更多更多的人，懷有熱情、堅定意志、把握時光、努力耕耘，別無他法。即使旅程的途中曾感到孤單與寂寞，也遇到不少卡關的事，但「放棄」從來就不是我的選項。別為了瑣碎的事、小小的錯誤而煩惱憂愁，就算是對方的賽末點也不代表比賽即將結束，失敗了也要有再站起來的勇氣，就當作是一場夢吧、睡一覺明天再重新開始吧，面對研究瓶頸或是人生轉折時，懂得將自我的心態適時地做些改變，應該是我在這段旅程中的最大收穫。

謝謝我的指導教授，楊偉勛老師，讓我有機會進入臨醫所就讀，對於整個研究在各方面都給予學生最大的幫助;謝謝實驗室的同事在生活上與實驗上的相互扶持;謝謝親朋好友們不管我這條路走了多遠、走了多久，依然一路義氣相挺。如今回頭看看自己所擁有的一切，當初若做了其他的選擇可能就遇不到這些美好的人事物，努力記得這美麗的風景吧，帶著大家對我的愛，繼續航向夢想的遠方。

陳彥婷

謹誌於 國立台灣大學臨床醫學研究所

中華民國一零八年七月

doi:10.6342/NTU201901578

中文摘要

內分泌系統為無導管腺體，藉由分泌激素去調控動物體內各種生理功能之正常運作，是維持體內恆定的重要控制系統。臨床上常見的內分泌疾病包括糖尿病、甲狀腺疾病以及肥胖症等，其中甲狀腺所分泌的甲狀腺素會去調控身體每個器官的新陳代謝，是極為重要的內分泌腺體。

S14 蛋白主要在會製造脂肪的組織表現，例如肝臟、乳腺和脂肪組織，參與脂肪酸合成，在大鼠肝臟中會被三碘甲狀腺激素(T3)大量誘發。然而，尚未有研究報告人血清中 S14 的存在及其甲狀腺功能狀態的關係。另外，動物實驗顯示 *S14* 基因發生缺失(deletion)時，小鼠對飲食誘導的肥胖和葡萄糖耐受具有更好的抗性，暗示 *S14* 基因在脂肪代謝中，扮演一定的角色。最近的研究顯示 S14 的傳訊核醣核酸(mRNA)在肥胖的個體中，其表達量減少，且禁食無法抑制其表達量，暗示 S14 可能參與肥胖及其共患疾病的病生理機轉，但目前尚未有研究探討人類血清中的 S14 與代謝相關因子之間的關聯性。我們利用自行開發的酵素免疫分析法偵測 S14 在血清中的濃度變化，探討 S14 作為生物標誌物應用於甲狀腺疾病、肥胖或是內分泌代謝相關疾病的可能性。

我們在臨床研究的第一部分，比較甲狀腺功能亢進症與甲狀腺功能正常患者的血清 S14 濃度並且評估血清 S14 與游離型甲狀腺素(fT4)或促甲狀腺激素(TSH)之間的關聯。我們招募了 26 名甲狀腺功能亢進患者和 29 名甲狀腺功能正常的人，分析 S14 和 fT4、TSH 或 TSH 四分位數之間的關聯。我們的分析顯示，甲狀腺功能亢進患者的血清 S14 濃度顯著高於甲狀腺功能正常的患者。在單變量線性回歸中，對數轉換的 S14 濃度（logS14）與 fT4 呈現正相關且與 TSH 或 TSH 四分位數呈現負相關。在多變量線性迴歸分析中，logS14 和 TSH 四分位數之間的負相關仍然顯著。我們的研究首先證實了甲狀腺功能狀態對人類血清 S14 濃度的影響。

我們臨床研究的第二部分招募了總共 327 名受試者，依據其是否有代謝症候群進行分類。我們的分析顯示，患有代謝症候群患者的血清 S14 濃度低於沒有代

doi:10.6342/NTU201901578

謝症候群的患者。代謝症候群、中心性肥胖、高三酸甘油酯、高密度脂蛋白低下和 logS14 之間存在負相關。我們的分析還揭示了年齡與 logS14 的負相關。這是第一篇探討人類代謝症候群與血清 S14 濃度是否相關的研究。

在基礎研究方面，S14蛋白的作用機轉目前還不明確，且S14在脂肪組織的研究仍然很少。然而，S14在脂肪組織之表現量其實是在各種組織中表現量最高的。我們發現隨著3T3-L1的分化，*S14*基因的mRNA表現量也會跟著上升。如果在3T3-L1前脂肪細胞(pre-adipocyte)中削弱*S14*基因的表現，會抑制脂肪細胞分化並影響其油滴的聚集。此外我們也發現許多參與在脂肪細胞分化途徑中重要的轉錄因子，例如 Krüppel-like factor 15(KLF15)以及過氧化物酶體增殖物活化受體(peroxisome proliferator-activated receptor gamma, PPARγ)也會因削弱S14基因表現而受到影響。我們也藉由免疫螢光染色的方式觀察到S14蛋白主要表現在3T3-L1前脂肪細胞的細胞核內，而在分化完成的脂肪細胞主要卻是表現在細胞質中。由於先前有研究顯示S14蛋白可能是一個轉錄因子或是轉錄共同激活因子，為了瞭解S14是否可以直接或是間接影響基因的轉錄，我們利用螢光素酶報告基因測定法(luciferase reporter assay)發現，相較於對照組，雖然KLF15以及PPARγ啟動子被激活的倍數不高，但在有S14表達載體的伴隨下還是有上升的趨勢。同時我們利用染色質免疫沉澱法(chromatin-immunoprecipitation, ChIP)合併高通量次世代定序(high-throughput next generation sequencing)以及一般的免疫沉澱法合併質譜儀分析(IP-Mass)去找尋S14蛋白可能作用的DNA序列以及直接或是間接有相互作用的蛋白質。此外，在本實驗室的前期研究當中發現當脂肪細胞處以促發炎的白細胞介素1β型(interleukin 1β, IL-1β)時，除了脂締素(adiponectin)這個與胰島素阻抗極為相關的因子的基因表現量會下降外，*S14*的基因表現也是極為顯著的下降。同時我們在這個研究當中也發現由衣黴素(tunicamycin)或是毒胡蘿蔔素(thapsigargin)所誘導的內質網壓力(endoplasmic reticulum stress, ER stress)同樣也會造成脂締素及S14 mRNA表現量下降。由於先前研究指出*S14*基因缺失的老鼠會有較好的胰島素敏感

doi:10.6342/NTU201901578

性，因此S14在發炎或是內質網壓力所引起的胰島素阻抗之調控也是未來我們想探討的議題之一。

為了進一步了解S14在脂肪組織的角色，我們與台灣大學基因體研究中心轉殖動物核心實驗室合作，利用CRISPR/Cas9 基因編輯技術將能轉錄出S14 蛋白質的外顯子前後插入loxp，並與由國家動物中心購入的脂締素-CreERT 老鼠配種，目的是選育出能針對脂肪組織施行特定時間剃除S14 基因的小鼠來釐清S14在脂肪組織的角色，這部分的實驗依然在進行當中。

綜合以上結果，本研究成功地開發可以測定人體血清中S14濃度的酵素免疫分析法，並且真實地應用在探討人體S14與甲狀腺功能以及代謝症候群之間的相關性。我們發現人體S14血清濃度與促甲狀腺激素成顯著負相關，此外，肥胖或是患有代謝症候群的患者其血中S14濃度顯著低於正常的組別，這些結果皆與前人的動物研究相呼應。我們希望未來這一套酵素免疫分析法能用來探討人類更多與胰島素阻抗或是脂肪生合成相關的疾病，例如第二型糖尿病或是非酒精性肝炎。同時，我們也藉由細胞實驗證實S14會參與在脂肪細胞分化以及油滴生合成的機轉當中，並且發現S14的確可能參與在發炎反應或是內質網壓力所誘發的胰島素阻抗，然而更詳細的機制還需要後續更多的研究來證實與闡釋。

中文關鍵字：內分泌系統、甲狀腺功能亢進、促甲狀腺激素、甲狀腺素、代謝症候群、中心性肥胖、高三酸甘油酯，高密度脂蛋白降低、酵素免疫分析法、脂肪細胞分化、發炎反應、內質網壓力。

doi:10.6342/NTU201901578

Abstract

Organs of endocrine system secret hormones, which circulate in blood, modulate physiological functions of end organs, and maintain body maintain homeostasis. Common endocrine disorders include thyroid dysfunction, diabetes mellitus, obesity, and etc. Thyroid which secrets thyroid hormones to affect rates of metabolism is a very important endocrine organ.

S14 protein is mainly expressed in lipid-producing tissues, such as liver, mammary gland and adipose tissue. *S14* is a thyroid hormone responsive gene which can be tremendously induced by T3, glucose, and insulin, and involves in fatty acid synthesis. However, the presence of S14 in human serum and its relation with thyroid function status have not been investigated. Compared to wild type, *S14* knockout mice had resistance to diet-induced obesity and better glucose tolerance. The mRNA expression of S14 in the adipose tissue of obese subjects was lower than the controls. It was suppressible by fasting in non-obese subjects but not in the obese subjects. These findings suggested that S14 may participate in the pathogenesis of obesity and its co-morbidities in humans. However, the associations between serum S14 level and metabolic variables in humans have never been investigated. We developed an enzyme-linked immunosorbent assay (ELISA) for S14, and explored the possibility of using S14 as a biomarker in thyroid or metabolic disorders.

doi:10.6342/NTU201901578

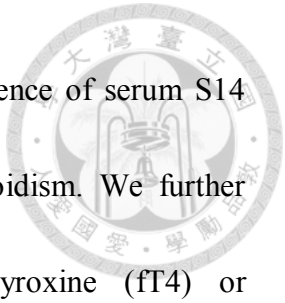

In the first part of our clinical study, we compared the difference of serum S14 concentrations between patients with hyperthyroidism and euthyroidism. We further evaluated the associations between serum S14 and free thyroxine (fT4) or thyroid-stimulating hormone (TSH) levels. Twenty-six hyperthyroid patients and 29 euthyroid individuals were recruited. Data of all patients were pooled for the analysis of the associations between the levels of S14 and fT4, TSH, or quartile of TSH. Our analysis revealed that the hyperthyroid patients had significantly higher serum S14 levels than the euthyroid subjects. In univariate linear regression, the log-transformed S14 level (logS14) was positively associated with fT4 and negatively with TSH or quartile of TSH. The negative associations between logS14 and quartile of TSH remained significant in multiple linear regression. Our study is the first to investigate the serum S14 levels in humans and the effects of thyroid function statuses on serum S14 levels.

The second part of our clinical study was designed to evaluate the associations between serum S14 concentrations with components of metabolic syndrome (MetS). A total of 327 subjects were recruited in this cross-sectional study and categorized by presence of MetS. Our analysis revealed that the patients with MetS had lower serum S14 levels than those without. Negative associations existed between MetS, central obesity, high triglyceride (TG), low high density lipoprotein C (HDL-C) and logS14.

doi:10.6342/NTU201901578

Our analysis also revealed a negative association of age with logS14. This is the first study to evaluate levels of S14 in patients with or without MetS.

In basic study, the exact function of S14 remains largely unclear and the studies of S14 in the adipose tissues are rare. However, the expression level of S14 in adipose tissue is the most abundant among all tissues. We found that after induction of 3T3-L1 with the cocktail of differentiation medium, S14 mRNA was up-regulated by more than 700-fold. We also found that knockdown of S14 by transducing lentiviral S14 shRNA reduced 3T3-L1 adipocyte differentiation and lipid accumulation. In addition, we also found that many transcription factors involved in adipocyte differentiation pathway, such as Krüppel-like factor 15 (KLF15) and peroxisome proliferator-activated receptor (peroxisome proliferator-activated receptor gamma, PPARγ) were affected by the knockdown of *S14* gene. According to the immunofluorescence staining data, we also observed that S14 protein is mainly expressed in the nucleus of 3T3-L1 pre-adipocytes, while mainly expressed in the cytoplasm in differentiated fat cells. Previous studies have shown that the S14 protein may be a transcription factor or co-activator. We tried to investigate whether S14 can directly or indirectly affect gene transcription. We performed luciferase reporter assay and found that the promoter activity of KLF15 and PPARγ with S14 overexpression constructs were slightly increased when compared to the control groups. We further used chromatin immunoprecipitation (ChIP) combined

doi:10.6342/NTU201901578

with high-throughput next-generation sequencing and general immunoprecipitation combined with mass spectrometry (IP-Mass) to search the potential S14 targeted-DNA sequences and potential S14 interacting proteins.

In our preliminary study, we found that the interleukin (IL) 1β-treatment was capable of reducing adiponectin level, as well as S14 expression. In this study, we found that tunicamycin or thapsigargin induced endoplasmic reticulum stress (ER stress) may trigger the mRNA expressions of adiponectin and decrease S14. Previous studies have shown that mice lacking *S14* gene have better insulin sensitivity. We intend to explore the regulation of S14 expression in inflammation or ER stress-related insulin resistance.

In order to understand the role of S14 in adipose tissue, we have been working on tissue specific conditional *S14* knockout mice under the service of Gene Knockout Mouse Core Laboratory of NTU enter of Genomic Medicine. We used CRISPR/Cas9 gene editing technology to insert loxp respectively at 5' and 3' to *S14* exon 1. Then we bred this strain with adiponectin-CreERT mice which was purchased from the Taiwan's National Laboratory Animal Center and selected to perform the adipose tissue-specific *S14* knockout strain to investigate the function of S14 in adipose tissue. This part of the experiment is still in progress.

Based on the above results, we successfully developed an enzyme immunoassay to measure the concentration of S14 in human serum, and applied it to explore the

doi:10.6342/NTU201901578

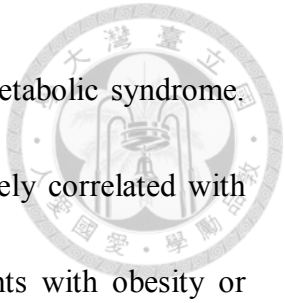

relationship between human S14 and thyroid function as well as metabolic syndrome. We found that the serum concentration of human S14 was negatively correlated with TSH. In addition, the concentration of S14 in the blood of patients with obesity or metabolic syndrome was significantly lower than that of normal subjects. These data are consistent with previous animal studies. We hope that in the future, this system can be used to explore more human diseases related to insulin resistance or fat synthesis, such as type 2 diabetes or non-alcoholic steatohepatitis. At the same time, we also confirmed by cell experiments that S14 participates in the adipocyte differentiation and oil droplet synthesis. We found that S14 may indeed involve in the inflammatory response- or endoplasmic reticulum stress- induced insulin resistance. However, the detail mechanisms require more investigations in the future.

Keywords: S14, endocrine system, hyperthyroidism, thyroid-stimulating hormone, thyroxine, metabolic syndrome, central obesity, high triglyceride, low high-density lipoprotein cholesterol, enzyme-linked immunosorbent assay, adipocyte differentiation, inflammatory response, endoplasmic reticulum stress.

doi:10.6342/NTU201901578

Table of Contents

doi:10.6342/NTU201901578

doi:10.6342/NTU201901578

doi:10.6342/NTU201901578

doi:10.6342/NTU201901578

doi:10.6342/NTU201901578

doi:10.6342/NTU201901578

doi:10.6342/NTU201901578

Chapter 1. Introduction

1.1 Endocrine system, thyroid disease, and metabolic syndrome

1.1.1 Endocrine system

The endocrine system refers to the cells, glands and organs that produce and secrete hormones directly into the blood in order to control physiological and behavioral activities, such as respiration, metabolism, reproduction, sensory perception, movement, sexual development and growth (Campbell and Jialal, 2019; Mollard and Schaeffer, 2018). The major glands of the endocrine system include pineal gland, pituitary gland, pancreas, ovaries, testes, thyroid gland, parathyroid gland, and adrenal glands (Mollard and Schaeffer, 2018). Some factors including aging, certain diseases, stress, the environment, and genetics can affect endocrine organs (Chrousos and Gold, 1992; Davidson et al., 1983; Thiessen and Rodgers, 1961). When the glands do not produce the right amount of hormones, either over or under, or the target cells do not respond properly to the stimulating of hormones, diseases can develop and affect many aspects of life (Wallymahmed et al., 1996).

1.1.2 Thyroid gland and thyroid diseases

The thyroid gland is a butterfly-shaped organ located at the base of the neck (Braverman, 2012). Thyroid gland secretes thyroid hormones including thyroxine (T4) and triiodothyronine (T3) and calcitonin. These thyroid hormones are important regulators of calcium homeostasis (Hirsch et al., 2001), energy expenditure (Silva, 2003), body weight (Knudsen et al., 2005), insulin resistance (Al-Shoumer et al., 2006; Maratou et al., 2010), lipid metabolism (Canaris et al., 2000; Pontikides and Krassas, 2007), and cardiac function (Biondi, 2012; Danzi and Klein, 2012). Hormonal output from the thyroid is regulated by thyroid-stimulating hormone (TSH) secreted from the anterior pituitary gland (Pirahanchi and Jialal, 2019). Thyroid dysfunction may cause

doi:10.6342/NTU201901578

several diseases. Hyperthyroidism is a condition in which the thyroid gland is overactive and makes an excessive amount of thyroid hormone (Campbell and Jialal, 2019). If there is too much thyroid hormone, every function of the body tends to speed up (Campbell and Jialal, 2019). Signs and symptoms vary among patients and may include nervousness, anxiety, fatigue, muscle weakness, rapid heartbeat, increased sweating, difficulty in sleeping, and weight loss (Campbell and Jialal, 2019). In contrast, hypothyroidism is a state of insufficient thyroid hormone production (Campbell and Jialal, 2019). In addition, the thyroid gland may also develop several types of nodule and cancer (Carling and Udelsman, 2014).

1.1.3 Obesity, chronic inflammation, ER stress, and insulin resistance

In many developing and developed countries, obesity has become an important public health issue (Wilkin and Voss, 2004). Genetic inheritance, excessive calories, and sedentary life habits contribute to the occurrence of obesity (Wilkin and Voss, 2004). Previous studies have shown that obesity will increased risks of type 2 diabetes mellitus (T2DM), cardiovascular disease, and certain types of cancer (Wilkin and Voss, 2004). Insulin resistance is one of the pathological responses of obesity (Wilkin and Voss, 2004). Insulin plays a key role in getting blood glucose into cells and responds promptly to postprandial glucose rising and stimulates glucose utilization by cells (Hardy et al., 2012). During the process of adipose tissue expansion, either with an increase of adipocyte number (hyperplasia) or increase in adipocyte cell size (hypertrophy), adipocytes as well as adipose tissue-resident immune cells would secrete pro-inflammatory cytokines, such as tumor necrosis factor alpha (TNF-α), interleukin 6 (IL-6), and IL-1β (Hardy et al., 2012; Ye, 2013). Although inflammation is a protective reaction in the body, persistent chronic inflammation may cause several adverse effects, such as macrophage infiltration, decreased insulin sensitivity, tissue injury, and organ

doi:10.6342/NTU201901578

dysfunction (Ye, 2013). On the other hand, endoplasmic reticulum (ER) stress is also involved in the development of insulin resistance (Salvado et al., 2015). The ER performs important functions related to the synthesis, folding and transport of proteins, and also plays a critical role in lipid synthesis and calcium homeostasis (Salvado et al., 2015). Any disturbance in these functions, referred as an "ER stress", will lead to the activation of a cellular response termed the unfolded protein response (UPR) (Flamment et al., 2012). Many studies have shown that UPR response is linked to different processes involved in the development of insulin resistance, such as lipid accumulation, insulin biosynthesis, inflammation, and β-cell apoptosis (Flamment et al., 2012). In order to overcome insulin resistance, pancreas would secret more insulin and thus result in hyperinsulinemia, which may secondarily cause hyperglycemia and diabetes mellitus (Hardy et al., 2012). Furthermore, insulin resistance and hyperinsulinemia may also impair fat metabolism, increase blood levels of triglyceride (TG) and low density cholesterol (LDL-C), decrease blood levels of high density of cholesterol (HDL-C), and induce coagulopathy or arteriosclerosis (Roberts et al., 2013). Obesity, impaired glucose and fat metabolism are major components of metabolic syndrome. Therefore, it is important to investigate the interactions among obesity, chronic inflammation, ER stress and insulin resistance in the context of metabolic syndrome.

1.1.4 Metabolic syndrome

Metabolic syndrome (MetS) is a cluster of several metabolic abnormalities (Kaur, 2014). MetS increases the risk for heart disease and other health problems, such as diabetes and stroke (Kaur, 2014). The prevalence of MetS in Taiwan is approximately 19.7% (male: 20.3%; female: 19.3%) (Hwang et al., 2006). The possible contributing factors of MetS include genetic defect, aging, physical inactivity, overweight or obesity, insulin resistance, chronic inflammation, and dysfunctional adipose tissue (Kaur, 2014).

doi:10.6342/NTU201901578

According to different ethnicity, the definition of MetS by different organizations is not exactly the same. In 1998, World Health Organization (WHO) firstly proposed the definition of MetS (Alberti and Zimmet, 1998). It emphasized the patients with MetS were ever diagnosed T2DM, impaired glucose tolerance, or insulin resistance and combined any two of higher waist-to-hip ratio/body mass index (BMI), higher TG/lower HDL-C, elevated blood pressure (BP), or microalbuminuria. On the other hand, in 2001, the National Cholesterol Education Program Adult Treatment Panel III (NCEP-ATP III) proposed that MetS was diagnosed with at least three components of the five constituted criteria, including elevated waist circumference, TG, BP, fasting glucose, and reduced HDL-C (Expert Panel on Detection and Treatment of High Blood Cholesterol in, 2001). In 2005, the American Heart Association/National Heart, Lung, and Blood Institute (AHA/NHLBI) subsumed the medical history of hypertension or the medications for elevated TG, BP, glucose, reduced HDL-C as components of MetS. Consideration of ethnic and gender difference, a lower cut-point of waist circumference ($\geqq$90/80 cm in male/female) was recommended for Asian population (Grundy et al., 2005). At the same year, the International Diabetes Federation (IDF) proposed a worldwide definition of MetS (Alberti et al., 2005). By the definition of IDF, a person having central obesity plus at least two components of raised TG, BP, fasting glucose, or reduced HDL-C can be diagnosed as MetS. A modification of the NCEP-ATP III definition of MetS was used in Taiwan (Hwang et al., 2006).

1.2 Adipocyte differentiation and lipid droplets accumulation

Adipose tissue is a special connective tissue mainly composed of adipocytes. Adipocytes store TG in lipid droplets, the main component of body fat, and provide structural support to protect organs (Frayn, 2001). There are two distinct types of

doi:10.6342/NTU201901578

adipose tissue, brown adipose tissue (BAT), which contains abundant of mitochondria and burns energy for thermogenesis, while white adipose tissue (WAT), is mainly responsible for energy storage (Coelho et al., 2013). Recently, adipose tissue has been recognized as an important endocrine organ because it produces various kinds of hormones that participate in energy homeostasis (Adamczak and Wiecek, 2013).

Adipocytes are derived from mesenchymal stem cells (Minteer et al., 2013). These multipotent stem cells commit to the fibroblast-like preadipocytes, undergo a series of morphological or biochemical changes, and then proceed to become adipocytes. This process is called adipogenesis (Tong and Hotamisligil, 2001). There are two major events of adipogenesis: preadipocyte proliferation and adipocyte differentiation, both of which involve activation or inhibition of many transcription factors (Tong and Hotamisligil, 2001). There are several stages in adipocyte differentiation. These include growth arrest of primary preadipocytes, confluent preadipocytes with clonal expansion, early gene expression and preadipocyte phenotype changed, and lipid droplets accumulation in terminal event (Gregoire et al., 1998).

1.2.1 Transcriptional control of adipocyte differentiation

Adipocyte differentiation involves a temporally regulated set of gene-expression events. Several transcription factor families, including the Krüppel-like factors (KLFs), CCAAT/enhancer binding protein (C/EBP), peroxisome proliferator-activated receptor (PPAR) and sterol regulatory element binding proteins (SREBP) families exhibit different modes of function, and serve as key regulators of the adipogenesis process (Rosen and Spiegelman, 2000; Tong and Hotamisligil, 2001).

In recent years, many members of KLF have been identified to be involved in both adipogenesis (Wu and Wang, 2013). Some of them promote adipogenesis and some may exert opposing effects. Activators of adipogenesis include KLF4, KLF5, KLF6, KLF9

doi:10.6342/NTU201901578

and KLF15, whereas KLF2, KLF3 and KLF7 inhibit adipogenesis (Wu and Wang, 2013).

After the treatment of preadipocytes with inducers of differentiation, C/EBPβ and C/EBPδ gene expression were rapidly increased (Darlington et al., 1998). Differentiating preadipocytes undergo approximately two rounds of cell division (mitotic clonal expansion) after differentiation is induced (Zhang et al., 2004). Then the pre-adipocytes exit the cell cycle and begin to express C/EBPα, which is followed by the induction of many genes involved in producing adipocyte phenotype (Darlington et al., 1998). Once expression is triggered, C/EBP can "auto-activate" its own gene and activate the expression of the other adipocyte genes thereby maintain adipocytes in the terminally differentiated state (Lane et al., 1999).

PPARs are ligand-activated transcription factors that belong to the nuclear hormone receptor super-family (Grimaldi, 2001). All three isotypes, α, β/δ and γ, were involved in the regulation of lipid and carbohydrate metabolism (Grimaldi, 2001). The level of PPARα in white adipose tissue and in adipocyte cell lines is very low, which suggests a limited role for this isotype during adipogenesis (Christodoulides and Vidal-Puig, 2010). In contrast, PPARβ/δ and PPARγ are upregulated during adipose conversion with differential time-course (Grimaldi, 2001). PPARβ/δ is already detectable in growing preadipocytes and is upregulated just at confluence to reach a maximal expression during the post-confluent proliferation (Grimaldi, 2001). The γ isoform is the master gene in adipogenesis, induced at the end of clonal expansion proliferation and is maximally expressed in terminally differentiated cells (Grimaldi, 2001).

SREBPs are a family of transcription factors that regulate cellular lipogenesis and lipid homeostasis by controlling the expression of many enzymes involved in the synthesis of cholesterol, fatty acid, TG and phospholipid (Ali et al., 2013).

doi:10.6342/NTU201901578

1.2.2 *De novo* fatty acid synthesis

De novo lipogenesis (DNL) or *de novo* fatty acid (FA) synthesis is the metabolic pathway that synthesizes fatty acids from excess carbohydrates in body (Ameer et al., 2014). These fatty acids can be incorporated into TG for energy storage. In animals and humans, the lipogenic pathway is active mainly in the metabolic tissues: liver and adipose tissue (Ameer et al., 2014). The flow of carbons from glucose to fatty acids includes a coordinated series of enzymatic reactions. Glucose is taken into cell cytosol by the glucose transporter then enters the glycolytic pathway and generates pyruvate (Ameer et al., 2014). Pyruvate is converted into acetyl-CoA by pyruvate dehydrogenase (PDH). Acetyl-CoA enters the tricarboxylic acid (TCA) cycle then citrate is produced and exits the mitochondria (Ameer et al., 2014). Citrate is then converted back into acetyl-CoA by the enzyme ATP-citrate lyase (ACLY) (Ameer et al., 2014). For fatty acid synthesis pathway, there are two central enzymes. First, the acetyl-CoA carboxylase (ACC) transfers the acetyl-CoA to malonyl-CoA (Ameer et al., 2014). Second, the fatty acid synthase (FAS) uses the malonyl-CoA to generate 16-carbon saturated palmitate (Ameer et al., 2014). After a series of reactions palmitate is further converted into complicated fatty acids.

The irregularity of DNL in the key lipogenic tissues could disrupt the usual lipid homeostasis in the body and cause many diseases, such as non-alcoholic fatty liver disease (NAFLD), obesity and insulin resistance (Ameer et al., 2014; Tamura and Shimomura, 2005).

1.3 S14 and S14R

1.3.1 S14 gene and its regulation

The S14 (Spot 14, also called thyroid hormone responsive protein, THRSP) was the

doi:10.6342/NTU201901578

14th spot of protein annotated on the two-dimensional gel for their differential expression in the thyroidectomized rat liver treated with or without T3 (Seelig et al., 1981). The *S14* gene can be greatly induced by T3, as well glucose and insulin (Jump and Oppenheimer, 1985). This gene is primarily expressed in lipid-producing tissues, such as liver, mammary gland and adipose tissue. Jump and Oppenheimer found that relative S14 mRNA expression levels in the fat depots and lactating mammary gland are respectively 10- and 4-fold higher than that in the liver of euthyroid male rat by Northern blot hybridization (Jump and Oppenheimer, 1985). In contrast, those in various non-lipogenic tissues, such as brain, heart, kidney, lung, spleen, testes, and pituitary are only 7% or less of that in the liver (Jump et al., 1984; Jump and Oppenheimer, 1985). S14 protein is an acidic protein (approximately 17 kDa and pI 4.65) bearing no sequence similarity to other well-recognized functional motifs, therefore it is unlikely to speculate its function simply based on its peptide sequences (LaFave et al., 2006).

1.3.2 S14 protein participates in lipid synthesis

In a previous study, rat hepatocytes were transfected with S14 antisense oligonucleotides. Compared with the controls, lipid synthesis as well as lipogenic enzymes, such as ACLY, FAS and malic enzyme, were reduced in antisense oligonucleotide transfected cells, implying its roles in lipogenesis (Kinlaw et al., 1995). Animal experiments showed that deletion of S14 dramatically reduced fatty acid synthesis in mammary gland (Zhu et al., 2005). However, whether S14 participates in lipid metabolism by regulating the transcription of key enzymes of fatty acids synthesis remains controversial (Kinlaw et al., 1995; LaFave et al., 2006). Some studies showed that S14 was translocated into nucleus upon T3 treatment and it interacted with thyroid hormone receptor (Chou et al., 2007). These suggest that S14 may act as a transcription

doi:10.6342/NTU201901578

factor or co-activator.

1.3.3 A paralog S14R may be redundant to S14 in lipid synthesis

In contrast to what was observed in the mammary gland of the *S14* knockout mice, lipid synthesis in the liver of these animals was not altered (Zhu et al., 2001). In fact, the data regarding the exact functions of S14 in lipid synthesis in the liver were contradictory. Knock-down of *S14* in primary hepatocyte culture showed reduced fatty acid synthesis with reduced activity of several enzymes, such as FAS and malic enzyme in lipid metabolism (Kinlaw et al., 1995). In contrast, deletion of *S14 in vivo* resulted in increased hepatic *de novo* lipogenesis (Zhu et al., 2001). After a long-term treatment with both T3 and a high-carbohydrate diet even led to enhanced lipogenic enzyme activity and a greater rate of hepatic *de novo* lipogenesis in the *S14* knockout mice, compared with the wild-type mice (Zhu et al., 2001). Zhu et al. proposed that a redundant pathway for lipid synthesis in the liver may rescue the *S14*-deficient phenotype (Zhu et al., 2005). This genetic redundancy may not exist in the mammary gland (Zhu et al., 2005). Later, a ubiquitously expressed paralogous protein named S14-related protein (S14R, also called midline 1 interacting protein 1 (MID1IP1) or MID1 interacting G12-like protein (MIG12)) was discovered (Berti et al., 2004; Zhu et al., 2005). S14R is 32% homologous to S14 in amino acid sequence. S14R encodes an approximately 22 kDa protein that was subsequently reported to cooperate with midline 1 (MID1) to bundle and stabilize microtubules (Kim et al., 2010). S14R was also reported to facilitate the polymerization of ACC, which catalyzes the first committed step in fatty acid synthesis (Colbert et al., 2010; Kim et al., 2010; Park et al., 2013). By doing so, the ACC activity was increased by 50x and the *de novo* fatty acid synthesis was increased. S14R is expressed at a very low level in the mammary gland, leading to the speculation that the reduced fatty acid synthesis in mammary gland in *S14*-deletion

doi:10.6342/NTU201901578

mice was secondary to the lack of compensation by S14R, the potential redundant gene in the liver (Aipoalani et al., 2010; Zhu et al., 2005). From the functional and structural studies, it was demonstrated that S14 forms heterodimers with S14R and prevent its facilitation of ACC polymerization (Colbert et al., 2010; Kim et al., 2010; Park et al., 2013). A model of S14 and S14R was also proposed to implicate the role of S14 and S14R in interaction with MID1 and microtubules as fatty acid trafficking proteins in lipid metabolism (LaFave et al., 2006). Co-expression of S14 with S14R actually attenuates the ability of S14R to activate ACC (LaFave et al., 2006). This observation suggests that the relative ratio between S14 and S14R may be critical for the biological role of S14 in lipid synthesis (Colbert et al., 2010).

1.3.4 S14 is associated with obesity and metabolic disorders

At the amino-acid sequence level, human S14 is 82% identical to mouse S14 (Zhang et al., 2011). The exact mechanisms of S14 function remain unclear. Lipid synthesis in the liver of *S14*-knockout mice did not decrease, whereas the knockout mice were resistant to diet-induced obesity with better glucose tolerance and insulin sensitivity (Anderson et al., 2009; Zhu et al., 2001). The lean mass of the knockout animals was not different from the wild-type animals, while both the white adipose tissue and brown adipose tissue were reduced (Anderson et al., 2009). In literature review, the function of S14 in human subject is seldom discussed. Only the mRNA in subcutaneous adipose tissue has been assayed (Kirschner and Mariash, 1999; Ortega et al., 2010). Unexpectedly, the basal S14 mRNA levels of obese subjects were lower than normal control (Kirschner and Mariash, 1999; Ortega et al., 2010). However, after 48-h fast, the S14 mRNA levels in the non-obese individuals, but not in the obese subjects were dramatically suppressed. This observation suggests that the expression of S14 in the adipose tissue of obese subjects is dysregulated and S14 may participate in the

doi:10.6342/NTU201901578

pathogenesis of obesity and its co-morbidity in humans (Kirschner and Mariash, 1999; Ortega et al., 2010).

In comparison to the liver and mammary gland, the role of S14 in the adipose tissues is not well characterized. Adipose tissue is the primary site of *S14* gene expression. The expression level of *S14* was reported to be 10x higher than that in liver (Harvatine and Bauman, 2006). The abundance of S14 mRNA in the adipose tissue was approximately 100-fold that of S14R, whereas it was only 10:1 in the liver (Harvatine and Bauman, 2006). S14 is documented in various adipocytes cell lines and human adipocytes and is activated during adipocyte differentiation (Hausdorf et al., 1988; Kinlaw et al., 1995; Ortega et al., 2010). In undifferentiated human preadipocytes, the expression level of S14 is low and S14 protein is mainly localized in the nucleus (Ortega et al., 2010). Once the adipocytes differentiated, S14 is abundant and localized in cytoplasm along with FAS (Ortega et al., 2010). These data suggest that S14 could be a multifunctional protein, performing different functions at different stages of adipocyte differentiation. On the other hand, the S14 mRNA expression in adipocytes or adipose tissue is regulated by various hormones (Table 1) (Blennemann et al., 1995; Clement et al., 1987; Freake and Moon, 2003; Freake and Oppenheimer, 1987; Jump and Oppenheimer, 1985; Kirschner and Mariash, 1999; Perez-Castillo et al., 1993).

As adipose tissue is the primary site of *S14* gene expression and the deletion of *S14* may result in resistance to diet-induced obesity and improvement in insulin sensitivity and glucose tolerance, to study the regulation and function of S14 in adipose tissue will be very helpful in understanding the pathogenesis of metabolic syndrome and related disorders such as obesity, dyslipidemia and NAFLD. S14 could potentially be a molecular target for treating these diseases.

doi:10.6342/NTU201901578

Chapter 2. Subjects, materials, and Methods

2.1 Clinical research

2.1.1 Human subjects

This thesis included two separate human study designs. Both studies followed the guidelines of the Declaration of Helsinki and were approved by the research ethics committee of the National Taiwan University Hospital (NTUH). Written informed consent was obtained from each subject.

[Spot 14 and Hyperthyroidism]

Patients with thyroid disorders at their first visit to the endocrinology clinics of NTUH during 2010 and 2011 were recruited in this study. We excluded the subjects who had medical history of thyroid disorders, other co-morbidities, or under medications. Consent was obtained from each of the 55 enrolled patients after providing a full explanation of the purpose, nature, and procedures of the study. The institutional review board (IRB) number for this study was 201005085R.

[Spot 14 and metabolic syndrome]

A total of 541 ostensibly healthy individuals who participated in a self-paid health check-up program at the Health Management Center (HMC) of NTUH were recruited. To eliminate the possible effects of inflammation and/or abnormal thyroid status, subjects with hyperthyroidism or hypothyroidism, any kind of inflammation or infection, such as acute illness, malignancy, hepatitis B, hepatitis C, rheumatoid arthritis, and systemic lupus erythematosus were excluded in this study. We also excluded people who were taking medicine for common cold, steroid, non-steroid anti-inflammatory drugs or thyroid therapy drugs. Finally, a total of 327 individuals were included for this study. The IRB number for this study was 201204030RIB.

doi:10.6342/NTU201901578

2.1.2 Data collection, measurement, and determination

General physical examination and blood chemistry were performed. Basic data such as age, gender, body height (BH), body weight (BW), body waist and blood pressure (BP) on the right arm were recorded. Body mass index (BMI) was calculated as BW in kilograms (kg) divided by BH in meters squared (m^2). Body fat percentage (BFP) was determined by using a body composition analyzer DX-300 (Jawon Medical, Gyeongsan, Korea).

Blood samples were drawn from antecubital vein after overnight fast for at least 8 hours. Postprandial plasma glucose (PPG) level of health checkup individual was examined 2 hours after taking a standardized meal (750 kcal, including 54% carbohydrates, 30% protein, and 16% fat) prepared by the nutrition room of HMC of NTUH (Hung et al., 2018). The blood chemistry data including alanine transaminase (ALT), aspartate transaminase (AST), creatinine (CRE), fasting plasma glucose (FPG), free thyroxine (fT4), hemoglobin (Hb), glycated hemoglobin (HbA1c), HDL-C, LDL-C, PPG, TSH, total cholesterol (T-C), TG, and uric acid (UA) were performed following the manufacturers' instructions of the routine tests by the Department of Laboratory Medicine, NTUH as previously described (Hung et al., 2015). Level of ALT and AST were determined by Hitachi 7080 biochemical analyzer (Hitachi, Japan). Level of FPG was measured using the Olympus AU series 680 with hexokinase method (Beckman Coulter, Nyon, Switzerland). Serum levels of T-C, TG, HDL-C and LDL-C were measured using the Olympus AU series 5800 with CHOD-PAP method, GPO-PAP method, accelerator selective detergent, and liquid selective detergent, respectively (Beckman Coulter, Nyon, Switzerland). TSH and fT4 were measured by Siemens DPC Immulite 2000 (Siemens, Erlangen, Germany). TSH-receptor antibody (TRAb) levels were determined by using the radioimmunoassay method (TSH receptor autoantibody

doi:10.6342/NTU201901578

coated tube kit, RSR, Cardiff, United Kindom). When the values were way outside the laboratory measurement range (fT4 level > 5.4 ng/dl or TSH level < 0.004 μIU/mL), they were recorded as fT4 level = 5.4 ng/dl or TSH level = 0.004 μIU/mL, respectively.

2.1.3 Patient groups and definition of disorders

[Spot 14 and Hyperthyroidism]

The data of TSH receptor antibody (TRAb), serum concentrations of fT4 and TSH and typical clinical manifestations of thyrotoxicosis were used to diagnose hyperthyroidism. The normal reference of fT4 and TSH used in NTUH were 0.6 to 1.75 ng/dL and 0.1 to 4.5 μIU/mL, respectively. Euthyroidism was defined as both fT4 and TSH levels within their normal reference ranges. When subject with the fT4 level > 1.75 ng/dL and the TSH level < 0.1 μIU/mL was defined as hyperthyroidism (Tseng et al., 2015). At the end, 26 subjects with newly diagnosed hyperthyroidism and 29 with euthyroidism were included for this study.

[Spot 14 and metabolic syndrome]

The modified criteria of metabolic syndrome (MetS) from National Cholesterol Education Program, Adult Treatment Panel III (NCEP ATP III) criteria for Asians were applied: (1) central obesity: waist circumference ≧ 90 cm in men and ≧ 80 cm in women; (2) elevated BP: BP ≧ 130/85 mmHg (SBP/DBP), diagnosed hypertension or known treatment for hypertension; (3) impaired fasting glucose: FPG level ≧ 100 mg/dl, diagnosed T2DM or known treatment for diabetes; (4) low HDL-C: serum HDL-C level < 40 mg/dl in men and <50 mg/dl in women; (5) high TG: serum TG level ≧ 150 mg/dl (Tan et al., 2004). MetS was diagnosed with at least three of the above five criteria, without any prerequisite. In our study, 98 subjects were diagnosed with MetS, and 229 subjects belonged to non-MetS.

doi:10.6342/NTU201901578

The cut-off points of high BFP for men were 25.0% and for women were 35.0% (Li et al., 2012).

2.1.4 Development of the enzyme-linked immunosorbent assay (ELISA) for human serum S14

A competitive indirect enzyme-linked immunoassay (ELISA) for human serum S14 was developed (Chen et al., 2016). Different reagents and working dilutions of antigen or antibody were tested. Polystyrene MaxiSorp® 96-well plates (Nunc A/S, Roskilde, Denmark) were coated with 100μl human recombinant S14 proteins (100 ng/ml, diluted in ice-cold 1x PBS; cat no. ag3721, ProteinTech, Chicago, IL) per well. The coated plates were sealed and incubated on an orbital shaker (at 100 rpm; OS701, KS, Taiwan) at 4℃ overnight. Next day, the solutions were discarded then washed with washing buffer [PBS-Tween (PBS-T), 0.05% Tween 20], and were pad-dried on a paper towel. Then the plates were blocked with 100μl blocking buffer (PBST with 1% BSA) each well, and incubated on the orbital shaker at 100 rpm at room temperature for 1.5 hours. The solution was discarded and then the plates were washed with PBS-T once and pad-dried on a paper towel. Subsequently, 50μl serum samples or standards were added in each well and incubated at room temperature on a rotor at 160 rpm. After one hour, 50μl rabbit anti-Spot 14 polyclonal antibody (diluted by 1:10000 in blocking buffer; catalog no. 13054-1-AP, ProteinTech, Chicago, IL) were added and incubated for 1.5 hours at room temperature and shaken at 160 rpm. After three times of washing with PBS-T, 100μl of horseradish peroxidase-conjugated goat anti-rabbit IgG polyclonal antibody (diluted in blocking buffer by 1:10000; GTX213110-01, Irvine, CA, USA) was added to each well and shaken (160 rpm) for one hour at room temperature. Following five times of washing with PBS-T, the solutions were then discarded and the plates were pad-dried on a paper towel. Then 100μl 3, 3', 5, 5'-Tetramethylbenzidine (TMB)

doi:10.6342/NTU201901578

solution (KPL, Gaithersburg, MD) were added to each well for coloration. After 15-minute incubation, the reaction was stopped by addition of 100μl 2.0 M H_2SO_4 per well. Immediately, the optical density of each well was read at 450 nm using microplate reader (VERSA max, Munich, Germany). The standard curve was obtained using four-parameter logistic model. The assay was validated by the determination of assay sensitivity, intra- and inter-assay variability. The minimum detection limit of the assay was 10 ng/ml. For the intra-assay variability, the coefficient of variance (CV) of six replicate sets of one serum sample was 7.5%. For the inter-assay variability, the CV of six independent assays of one serum sample was 9.5%.

2.1.5 Statistical analysis for clinical data

[Spot 14 and Hyperthyroidism]

We presented the numerical variables as median values (Q1, Q3) and used Mann-Whitney U test to compare the numerical variables between the hyperthyroidism and euthyroidism groups. Categorical data were presented as percentage. Fisher's exact test was used for comparisons of categorical variables. The skewness and kurtosis of the data was checked with normality test. We made log transformation of S14 levels for analysis. To analyze the possible associations between logS14 levels and other variables, the data of the patients with hyperthyroidism or euthyroidism were pooled together. Log transformation of serum levels of S14 (logS14) was calculated. The effects of demographic, anthropometric, or laboratory parameters for logS14 were evaluated by performing linear regression analyses.

To minimize the possible bias that might exceed the range of the commercial kits, we divided the TSH into quartiles (Group 1: TSH $\leqq$ 0.004; Group 2: 0.004 < TSH $\leqq$ 0.422; Group 3: 0.422 < TSH $\leqq$ 1.17; Group 4: 1.17 < TSH). The effect of TSH

doi:10.6342/NTU201901578

quartile group for logS14 was also calculated by regression analysis.

We performed stepwise forward multivariate regression to analyze the effects of demographic, anthropometric, or laboratory parameters for logS14 concentrations. Only variables with *P* values < 0.05 were considered as statistically significant.

[Spot 14 and metabolic syndrome]

All numerical data were expressed as mean ± standard deviation (SD). Differences of serum S14 levels between subjects with or without specified anthropometric or metabolic factors were analyzed by using *t* test. Differences of categorical data between groups were analyzed by Chi-square test. We used the skewness and kurtosis of the data to check the normality and made log transformation of S14 levels for analyzing the associations with demographic, anthropometric, or laboratory parameters by linear regression. To estimate the odds ratios (OR) of metabolic syndrome and its different components in relation to logS14, we divided the logS14 into quartiles. Logistic regression models were used with the adjustment of age and gender to examine the OR with 95% confidence intervals (CI). *P* values < 0.05 were considered as statistically significant. All statistical analyses were conducted using IBM SPSS version 22.0 statistical package (IBM Corporation, Armonk, USA).

2.2 Cell and molecular biology

2.2.1 3T3-L1 pre-adipocyte culture and differentiation

3T3-L1 mouse pre-adipocytes have been widely used to study adipocyte biology. 3T3-L1 pre-adipocytes were purchased from the American Type Culture Collection (ATCC, CL-173^{TM}) and grown in Dulbecco's Modified Eagle Medium (DMEM) with high glucose (4.5 g/L) supplemented with 10% (v/v) newborn calf serum (NBCS). The cell culture was maintained in a humidified incubator at 37℃ with 5% CO_2. For

doi:10.6342/NTU201901578

differentiation, confluent cells were cultured for additional two days and next with an induction medium of DMEM supplemented with 10% fetal bovine serum (FBS), 1 μM dexamethasone (DEX), 0.5 mM 3-isobutyl-1-methylxanthine (IBMX) and 1 μg/ml insulin. Two days later, the induction medium was replaced with maintenance medium (DMEM with 10% FBS and 1 μg/ml insulin) and the medium was changed every two days until fully differentiated.

2.2.2 Spot 14 knockdown by lentiviral transduction

The pLKO.1-shS14 plasmid, which encodes short hairpin RNA targeting S14, was obtained from the National RNAi Core Facility at Academia Sinica at Taipei. The sequences of S14 shRNA were 5'-CCCTGATCTCTATACCTACTT-3' (TRCN000095920). The pLKO.1-shLuc (TRCN0000072249) targeting the luciferase gene was used as a control for RNA interference. For lentiviral transduction, the 3T3-L1 pre-adipocytes were seeded at approximately 40% confluence in 10-cm dishes one day prior to transduction. Next day, 7 ml fresh medium containing polybrene (10 μg/ml) and S14 shRNA or control lentivirus at appropriate titers ($8x10^7$ R.I.U virus, M.O.I=8) were added to each well. The curve of transduced cells' viability versus viral dose was used to estimate the relative titer of lentivirus following the manufacturer's instruction. Forty-eight hours later, the infected cells were switched to medium containing puromycin (2 μg/ml) for selection for another two weeks. The stably transduced cells were induced to differentiation as described above.

2.2.3 Oil red O staining

In 1 ml isopropanol, 3.5 mg Oil Red O (Sigma-Aldrich, St. Louis, MO) was dissolved and filtered with a 0.22 μm filter, and stood at room temperature as the stock solution. The Oil Red O working solution was freshly prepared (60% v/v stock and 40% v/v ddH_2O) before staining. Adipocytes were washed with PBS and fixed with 10%

doi:10.6342/NTU201901578

formaldehyde at room temperature for 10 minutes, followed by another one hour with 10% formaldehyde. Then the cells were washed twice with PBS and once with 60% isopropanol. After washing, the plates were placed into a 50°C oven for 15 minutes to dry the residual solvent completely, followed by staining with Oil Red O working solution for 20 minutes at room temperature. After washing with distilled water four times, the amount of lipid can be estimated by photograph immediately under a microscope. Alternatively, the Oil Red O coupled with the lipid can be eluted with 100% isopropanol and measured at 492 nm by a spectrophotometer (VERSA max, Munich, Germany).

2.2.4 RNA extraction, RT-PCR, and real-time PCR

Total RNA of 3T3-L1 cells and animal tissue samples were extracted using TRIzol reagent (Ambion, Texas, USA) and followed by reverse transcription by a RT kit (Fermentas/Thermo Scientific, St. Leon-Rot, Germany) following the manufacturer's instruction. The relative mRNA levels for specific genes were quantified by real-time qPCR using ABI StepOne Plus detection system (Applied Biosystems, Foster city, USA) and Roche LightCycler 480 (Roche Diagnostics, Mannheim, Germany). The primer sequences of the relevant genes for qPCR were listed in Table 2, and the melting points (Tm) of these primer pairs are all 60 °C. The expression levels of the examined genes were normalized to 36B4 expression.

2.2.5 Cytokines and ER stress inducers treatment

Adipocytes were treated with 10 ng/ml IL-1β (Peprotech, Rocky Hill, NJ) or 10 ng/ml TNF-α (Biovision, Inc., Milpitas,CA) to trigger inflammation and 100 nM Thapsigargin (Tocris Bioscience, Bristol, UK) or 1 μg/ml Tunicamycin (Sigma-Aldrich, Steinheim, Germany) to induce ER stress for 24 hours. All the inhibitors for blocking different signaling pathways used were summarized in Table 3.

doi:10.6342/NTU201901578

2.2.6 Protein extraction and Western blot analysis

The 3T3-L1 cells were washed with ice-cold PBS twice. Then the cells were lysed in radio-immunoprecipitation assay lysis buffer (RIPA buffer: 30mM Tris-HCL, 150mM NaCl, 1% Triton X-100, 1% sodium deoxycholate, 0.1% SDS in ddH_2O) with protease inhibitor cocktail (Roche, Penzberg, Germany) and incubated on ice for 30 minutes. After centrifugation (12000 rpm, 4℃, 30 minutes), the supernatant were harvested as total cellular protein lysate. Protein concentration was measured by a BCA protein assay kit (Pierce, Bonn, Germany). For SDS polyacrylamide gel electrophoresis (PAGE), cell lysates were boiled with 1x sample buffer with 5% beta-mercaptoethanol (β-ME, Sigma-Aldrich, St. Louis, USA). Boiled lysates of 10-50 μg were electrophoresed on a 12 or 15% SDS-PAGE gel in Tris-Glycine buffer system and transferred onto 0.22 μm nitrocellulose membranes (Sartorius-Stedim Biotech, Göttingen, Germany) in Tris-Glycine-Methanol buffer. The membrane was blocked with 1x Tris-buffered saline with 0.1% Tween-20 (TBST) containing 5% bovine serum albumin (BSA) or nonfat milk, followed by incubation respectively with rabbit anti-THRSP polyclonal antibody (Abcam, Cambridge, UK, ab97504, 1:1000), rabbit anti-THRSP polyclonal antibody (GeneTex, Irvine, USA, GTX32922, 1:1000), goat anti-THRSP polyclonal antibody (R&D Systems, Minneapolis, MN, USA, AF6574, 1:400), and rabbit anti-beta-actin polyclonal antibody (GeneTex, Irvine, USA, GTX109639, 1:10,000) as indicated in each experiment on an orbital shaker at 4℃ overnight. Then the membrane was washed three times with 1x TBST and incubated with horseradish peroxidase (HRP)-linked goat anti-rabbit IgG polyclonal antibody (GeneTex, Irvine, USA, GTX213110-01, 1:10,000) for 1 hour at room temperature. After the membrane was washed thrice with 1x TBST, the signals were quantified by an enhanced chemiluminescence (ECL) detection system

doi:10.6342/NTU201901578

(GE Healthcare, Little Chalfont, UK).

2.2.7 Immunofluorescence stain

Fibroblasts or adipocytes were grown on glass coverslips (18 x 18 mm) and fixed with 2% (v/v) formaldehyde in PBS. All fixed cells were quenched with quench buffer (PBS containing 0.1% Triton X-100 and 150 mM sodium acetate, pH 7.4). Cells were then washed with wash buffer (PBS containing 0.1% Triton X-100), followed by blocking with blocking buffer (wash buffer containing 3% BSA) and subsequently incubated with primary antibody for overnight at 4℃. After wash, cells were then incubated with the species-specific fluorophore-conjugated secondary antibody (Jackson ImmunoResearch, West Grove, PA, USA) for 1 hour at room temperature. To stain the lipid droplets of adipocytes, cells were incubated with BODIPY 493/503 (D3922, Invitrogen, Carlsbad, CA) for 10 minutes at room temperature. All cells were incubated with 0.5μg/ml 4', 6-diamidino-2-phenylindole (DAPI; Sigma-Aldrich, St. Louis, USA) for nuclear staining and mounted with Fluoromount-G mounting medium (SouthernBiotech, Birmingham, AL, USA). Traditional fluorescence microscopy images were collected using an OLYMPUS IX70 fluorescence microscopy. Images from confocal microscopy were collected using a Leica TCS SP5 confocal microscopy.

2.2.8 Luciferase assay

One day prior to transfection, 3T3-L1 fibroblasts were seeded onto 6-well culture dishes (8 x 10^4 cells per well) were co-transfected with the 1 μg pGL3-KLF15 or pGL3-PPARγ promoter plasmids with 1 μg pcDNA3.1-S14 and 10 ng *Renilla* luciferase vector with TurboFect Transfection Reagent (Thermo Scientific, St. Leon-Rot, Germany). On day 6 after the induction of differentiation, adipocytes were also co-transfected with the same plasmids as 3T3-L1 fibroblasts. After 48-h incubation, the firefly and *Renilla* luciferase activity were determined by Dual Luciferase Reporter

doi:10.6342/NTU201901578

Assay System (Promega, Mannheim, Germany) according to the manufacturer's instructions. The samples were detected in a Plate Chameleon Luminometer (Hidex, Turku, Finland)

2.2.9 Chromatin immunoprecipitation (ChIP)

ChIP assays were performed according to manufacturer's protocols (#91820, Cell Signaling Technology, Danvers, USA). Briefly, 3T3-L1 fibroblasts were fixed with 1% formaldehyde at RT for 10 minutes. Then quenching unreacted formaldehyde with glycine at RT for 5 minutes, following wash with ice-cold PB and lysing cells with nuclear lysis buffer. The lysate were sonicated on Sonicator® (XL2020, Misonix, Farmingdale, NY, USA) at middle power setting for 3 cycles (each cycle: on 20 sec and off 20 sec for 5 minutes). After centrifugation (9400g, 10 minutes, 4℃), the supernatant was transferred to a new tube. The length of sheared DNA was determined by 1% agarose gel and was about 150-900 base pairs (bp) (Figure 1). The antibody against IgG (GeneTex, Irvine, USA), Histone H3 (Cell signaling Technology, Danvers, USA), THRSP (R&D Systems, Minneapolis, MN, USA) were used to immunoprecipitate DNA fragments. The precipitated DNAs were analyzed by PCR (GeneAmp® PCR system 2700, Applied Biosystems®, Waltham, USA).

2.2.10 Transient transfection, Immunoprecipitation and Mass spectrometry

We used HEK293 human cell line for analyzing S14 protein and other potential protein interaction. HEK293 cells were transiently transfected with 2 μg pcDNA3.1 empty vector or pcDNA3.1-Spot 14-Flag plasmids by TurboFect Transfection Reagent (Thermo Scientific, St. Leon-Rot, Germany). The Flag-tagged S14 protein and its interacting partners were isolated form cell extracts by immunoprecipitation using M2-Agarose resin (Sigma-Aldrich, St. Louis, USA). Briefly, the 500μg of total protein extracts were first incubated with 5μg of agarose beads for 60 minutes at 4℃ the

doi:10.6342/NTU201901578

centrifuged at 4000*g* for 5 minutes to remove nonspecific binders. The supernatant was incubated with 5μg of anti-Flag monoclonal antibody covalently attached to crosslinked agarose beads (M2). The mixture was gently mixed by inversion on a multi-rotator (25rpm, Multi Bio RS-24, Biosan, Riga, Latvia) for overnight at 4℃. The insoluble fraction were recovered by centrifugation (4000*g* for 3 minutes) and washed by five cycles of resuspension in wash buffer (20mM Tris-HCl, 250mM NaCl, 1% Triton X-100, pH7.4) followed by centrifugation as described above. Immunocomplexes were eluted from the beads by resuspension in 60μl of 2x SDS samples buffer containing β-ME and boiled for 10 minutes. One third of supernatant was used for Western blot analysis to check the S14 protein. The remaining extracts were used for SDS-PAGE analysis and stained with coomassie blue. The protein bands of interest were excised for in-gel digestion with trypsin and chymotrypsin. The resulting peptides were analyzed by tandem mass spectrometry. We send the samples to Dr. Pang-Hung Hsu's Lab in the Department of Bioscience and Biotechnology of National Taiwan Ocean University for performing Mass and data analyzing. All MS/MS spectra were converted to the mgf format and analyzed by MassMatrix software.

2.2.11 Statistical analysis for basic research

Statistical analysis was indicated in each corresponding figure legend. All data were generally presented in mean ± SD from at least 3 independent assays. All analyses were calculated using Excel (Microsoft Office 2013). *P* values were calculated from two-tailed statistical tests. A difference is considered statistically significant when $p < 0.05$.

2.3 Animal model establish

S14 gene has two exons and the coding region only resides in the first exon. In order

doi:10.6342/NTU201901578

to investigate the specific role of S14 in animal model, we used the Gene Knockout Mouse Core Laboratory of NTU Center of Genomic and Precision Medicine to create conditional *S14* exon 1 deletion mice by CRISPR/Cas9 strategy (Figure 2). Briefly, we inserted *loxp* respectively at 3676 bp 5' to S14 exon 1 and 445 bp 3' to S14 exon 1 by CRISP/Cas9 strategy. Mouse ES cells were transfected with the plasmids expressed Cas9 and target specific sgRNAs. The sequence of S14 5'sgRNA was 5'-CAACTGCCGAGCGTGTCATT-3' and S14 3'sgRNA was 5'-GGGCATACATGGCGTGCTCT-3'. Thirty-two mice were bred. Only 2 founders with the targeting sequences were identified by sequencing. The sequences of primers for genotyping as following: 5VF1 16314 (5'-TGACGTTAACACCTGTTTGGAGT-3'), 5VR1 16857 (5'-GGAACCATTTACCCCATCTCCTG-3'), 3VF1 20890 (5'-GTGACCTCCTACAGAGGACAGAA-3'), and 3VR1 21376 (5'-TGAGGCAGAAGAATCTCTACGTT-3').

In order to generate the adipose tissue specific *S14* knockout mice, we bought a strain of mice, C57BL/6-Tg(Adipoq-FusRed,-cre/ERT2)13Narl, from National Laboratory Animal Center. The strain was generated by microinjection of C57BL/6J embryos with Adipoq-FusRed-IRES-cre/ERT2 (BAC base) transgene and the Cre recombinase will express in adipose tissue and activates after tamoxifen treatment (Figure 3). Tamoxifen (T5648, Sigma-Aldrich, St. Louis, USA) was dissolved in corn oil (C8267, Sigma-Aldrich, St. Louis, USA) at a concentration of 20 mg/ml. To induce Cre recombinase activity, transgenic mice were injected intraperitoneally with tamoxifen (1-1.5mg/20g body weight) for five consecutive days. Mice were dissected at 28 days after treatment and tissue samples were collected. The sequences of primers for genotyping as following: CreF (5'-CTAAACATGCTTCATCGTCGGTC-3') and CreR (5'-TCTGACCAGAGTCATCCTTAGCG-3').

doi:10.6342/NTU201901578

Animal protocols were approved by the Institutional Animal Care and Use Committee, Colleges of Medicine and Public Health of National Taiwan University in accordance with National Institutes of Health guidelines (IACUC application no. 20140555). All animals were housed at an ambient temperature with a 12 hours light/dark cycle and were fed with a standard rodent diet at libitum and provided free access to water.

doi:10.6342/NTU201901578

Chapter 3. Results

3.1 Clinical research

3.1.1 Patients with hyperthyroidism had higher serum S14 levels

This study enrolled 26 subjects with hyperthyroidism (34.6% were males) and 29 with euthyroidism (13.8% were males) (Table 4). The anthropometric characteristics and laboratory data of hyperthyroid and euthyroid patients at their first visit are shown in Table 4. The median value of age of the patients with hyperthyroidism and euthyroidism was 35.5 and 43 separately (Table 4). The subjects with hyperthyroidism had higher fT4, AST and ALT levels but lower TSH, CRE, T-C, HDL-C, and LDL-C levels than the euthyroid patients (Table 4). The FPG and TG levels of patients with hyperthyroidism were higher, but not statistically significant, than those of subjects with euthyroidism. The median S14 levels of hyperthyroid patients were higher than those of euthyroid subjects (975 [669, 1612] ng/mL vs 436 [347, 638] ng/mL, $p < 0.001$; Table 4). The difference of S14 levels between hyperthyroidism and euthyroidism was only significant in females, not in male (Table 4).

3.1.2 Serum S14 concentration is negatively associated with TSH level

The predictive effects of demographic, anthropometric, or laboratory parameters for S14 concentrations were evaluated by performing a linear regression analysis. The univariate linear regression analysis revealed that logS14 was negatively associated with CRE ($\beta = -1757$, $p = 0.006$), T-C ($\beta = -0.006$, $p = 0.004$), TG ($\beta = -0.004$, $p = 0.015$), LDL-C ($\beta = -0.007$, $p = 0.015$), and TSH ($\beta = -0.371$, $p < 0.001$) (Table 5) in all patients. In addition, logS14 was positively associated with fT4 ($\beta = 0.213$, $p = 0.003$) (Table 5). After adjustment with age and sex, the association between logS14 and CRE, T-C, TG, fT4, TSH remained significant ($\beta = -2.681$, $p < 0.001$; $\beta = -0.006$, $p = 0.023$; $\beta = -0.004$, $p = 0.029$; $\beta = 0.192$, $p = 0.010$; and $\beta = -0.340$, $p = 0.003$, respectively) (Table 5).

doi:10.6342/NTU201901578

However, the association between logS14 and LDL-C became insignificant. In addition, the significant associations between logS14 and age, BW, BMI, CRE, AST, TC, TG, LDL-C, fT4, and TSH were only existed in females but not in males (Table 5). We divided the TSH into quartiles (Group 1: TSH $\leqq$ 0.004; Group 2: 0.004 < TSH $\leqq$ 0.422; Group 3: 0.422 < TSH $\leqq$ 1.17; Group 4: 1.17 < TSH). The TSH quartile group was also negatively associated with logS14 level (β = -0.302, $p < 0.001$) in the linear regression analysis (Table 5 and Figure 4). The stepwise multivariate regression analysis shown that TSH quartile group was still negatively related to the logS14 level (Table 6).

3.1.3 Demographics and characteristics of human subjects in MetS study

In a total of 327 subjects, the mean age was 53.2 years old and 61.5% were males (Table 7). Ninety-eight subjects of them (30.0%) were diagnosed with MetS (Table 7). About 36.8% in males and 19.0% in females had MetS. The mean age of the subjects with MetS were slightly higher, but not significantly, than that of without MetS (non-MetS) (54.2±8.4 years vs. 52.8±10.2 years, p = 0.183, Table 7). There were significantly more males in MetS group than non-MetS group (75.5% vs. 55.5%, $p<0.001$, Table 7). The subjects with MetS had significantly higher BH, BW, BMI, BFP, waist, pulse, SBP, DBP, ALT, FPG, PPG, CRE, Hb, HbA1c, TG, and UA, but lower HDL-C in comparison to those without (Table 7). There was no difference of thyroid function tests (fT4 and TSH) between these two groups.

3.1.4 The subjects with MetS had lower serum S14 levels

The mean serum S14 level of total subjects was 101.2±37.7 ng/ml. By two-tailed independent t-test, it was found that the mean S14 level of female subjects was significantly higher than that of male subjects (112.7±42.9 ng/ml vs. 94.0±32.1 ng/ml, $p<0.001$). The subjects with MetS had significantly lower S14 levels than that of the

doi:10.6342/NTU201901578

non-MetS subjects (87.1±26.3 ng/ml vs. 107.3±40.2 ng/ml, p<0.001) (Table 7, Figure 5).

Analysis with consideration of each component of the MetS criteria revealed that the subjects with central obesity (95.7±30.4 ng/ml vs. 107.0±43.4 ng/ml, p = 0.006) and high TG (87.2±26.3 ng/ml vs. 106.1±39.8 ng/ml, p<0.001) had significantly lower serum S14 levels than those without (Figure 5). In addition, the subjects with low HDL-C also had significantly lower S14 levels than those without (94.2±31.3 ng/ml vs. 104.6±40.0 ng/ml, p = 0.02) (Figure 5). There were no significant differences in S14 levels between the subjects with and without elevated BP or with and without impaired fasting glucose (IFG) (Figure 5). On the other hand, the subjects with high body fat (93.3±33.9 ng/ml vs. 106.1±39.1 ng/ml, p = 0.003) or BMI (87.6±31.8 ng/ml vs. 104.5±38.3 ng/ml, p = 0.001) also had significantly lower S14 levels than those without (Figure 5).

3.1.5 Serum S14 level was negatively correlated with metabolic profiles in multivariate linear regression analysis

In univariate linear regression analyses, logS14 was significantly related to age in a negative manner (β = -0.004, p = 0.029). Female gender was significantly associated with higher logS14 (β = 0.177, p<0.001). Adjusted with age and gender, MetS was negatively related to logS14 (Table 8). Using individual component of the MetS as the independent variable, logS14 had negative association respectively with central obesity, low HDL-C, and high TG (Table 8). In contrast, the relationship between logS14 and elevated BP or IFG was not significant (Table 8). In multivariate linear regression with adjustment of age, gender and all five components of the MetS as independent variables in the model, age (β = -0.120, p = 0.030), gender (β = -0.237, p<0.001), central obesity (β = -0.139, p = 0.016) and high TG (β = -0.152, p = 0.011) were significantly

doi:10.6342/NTU201901578

associated with the logS14 levels in a negative manner (Table 9). In contrast, there was no significant between logS14 and elevated BP, IFG or low HDL-C (Table 9).

3.1.6 Higher S14 level associated with reduced risk of MetS

In binary logistic regression models, the ORs for the MetS and its five diagnostic components were respectively evaluated with quartile of logS14 adjusted with age and gender. The increment in logS14 level reduced risk for MetS, central obesity, low HDL-C, or high TG with a dose response trend (Table 10). Each quartile increment in logS14 was associated with reduced risk for the MetS (OR 0.65, 95% CI, 0.51–0.82, $p<0.001$), central obesity (OR 0.72, 95% CI, 0.58–0.89, $p = 0.002$), low HDL-C (OR 0.76, 95% CI, 0.61–0.95, $p = 0.015$) and high TG (OR 0.65, 95% CI, 0.51–0.83, $p = 0.001$) respectively by 35%, 28%, 24% and 35%. On the other hand, the risk for elevated BP and IFG had no difference from various logS14 levels.

3.2 Basic research

3.2.1 Establish an immune related insulin resistant cell model

Differentiation of 3T3-L1 fibroblasts into adipocyte-like cells is the most common *in vitro* model used in the study of adipocyte biology (Green and Meuth, 1974). In order to study the pathological mechanism of immune related insulin resistance, we treated 3T3-L1 adipocytes with inflammatory cytokine IL-1β and found that the mRNA expression level of adiponectin, an adipocyte-derived hormone, was repressed in our lab's preliminary experiments. This result demonstrated that inflammatory response really influenced adipocyte function. Following, we performed gene microarray for analyzing the gene expression differences between 3T3-L1 adipocytes which were treated with and without IL-1β. The expression of certain genes were significantly altered by more than 2-fold in IL-1β treated cells genes were further confirmed by

doi:10.6342/NTU201901578

real-time PCR (Table 11). According to the data, S14 was the most significantly down-regulated gene in IL-1β treated cells compared with the controls. So far we only know that S14 was involved in fatty acid synthesis, but the detailed mechanism and the role of S14 in fat cells remain unclear.

3.2.2 S14 and S14R are activated during adipocyte differentiation

In order to study the function of S14 in adipocytes, we used 3T3-L1 cell as a model and observed the expression of S14 during adipocyte differentiation. After induction with the cocktail of insulin, dexamethasone (DEX), and 3-isobutyl-1-methyl-xanthine (MIX) at day 4, the S14 mRNA was up-regulated up to more than 400-fold, and even up to 700-fold on day 8 during 3T3-L1 differentiation (Figure 6a). In contrast, S14R, the paralogous gene of S14, was enhanced only by less than 3-fold in the same experiments (Figure 6b). The result suggested that compared with S14R, S14 may play a more important role in adipocyte differentiation.

3.2.3 S14 is necessary for adipocyte differentiation

To further address the function of S14 in adipogenesis, we knocked down S14 mRNA expression using specific shRNA. In 3T3-L1 pre-adipocytes, infection with the lentivirus containing S14-shRNA significantly decreased S14 mRNA by 50% compared with the scramble controls (Figure 7a). In contrast, the S14R and adiponectin mRNA levels were not affected by S14-knockdown in pre-adipocytes (Figure 7a). Interestingly, after adipogenic induction, the S14 mRNA level in the cells infected with S14-shRNA lentivirus was only 12% that of the differentiated adipocytes infected with the scramble controls (Figure 7b). The adiponectin mRNA level was profoundly decreased by S14 silencing as well (Figure 7b). However, the S14R mRNA level was not affected. The S14-shRNA infected cells did not appear to differentiate well and therefore accumulated far less lipid droplets compared to the scramble control cells (Figure 7c). Quantification

doi:10.6342/NTU201901578

of triglycerides by Oli-Red-O dye eluted from the cells indicated that the lipid accumulation was reduced by 89% with S14-knockdown compared to the controls (Figure 7d). These results suggest that S14 plays a role of adipogenesis and that S14R is unable to complement the loss of S14 in adipocyte differentiation (Figure 7).

3.2.4 Knockdown S14 affects the adipocyte differentiation gene markers

To determine the possible mechanism by which S14 may affect 3T3-L1 differentiation, we assayed the expression levels of various genes at different stages related to adipocyte differentiation in 3T3-L1 cells infected with S14 shRNA or scramble RNA lentiviruses at undifferentiated or differentiated stages. Neither activators nor suppressors of the pre-induction phase were significantly altered by S14-knockdown (Figure 8). Among the genes in the early phase of adipogenesis, C/EBP homologous protein 10 (CHOP10), a dominant-negative member of the C/EBP family, was decreased to 40% of the controls, whereas KLF15, a pivotal activator of adipogenesis, was down-regulated to only 13% (Figure 8b, 8c). Among the genes in the late phase of adipogenesis, C/EBPα was reduced to 15% (Figure 8c). Since both KLF15 and C/EBPα are the transcription factors upstream to PPARγ2 in adipogenesis, the mRNA of PPARγ2 was reduced to only 10% by down-regulation of the S14 expression compared to the scramble control in differentiated adipocytes (Figure 8c). We also measured some other genes expressed at the terminally differentiated stage, such as adiponectin (ADQ), fatty acid binding protein 4 (FABP4), resistin (RETN), hormone-sensitive lipase (HSL), lipoprotein lipase (LPL), acetyl-coA carboxylase (ACC), and fatty acid synthase (FAS) (Ranganathan et al., 2006; Strable and Ntambi, 2010). Their mRNA levels were all profoundly reduced by S14 knockdown (Figure 8c). These observations suggest that S14 regulates adipogenesis and lipogenesis.

3.2.5 Different intra cellular locations of S14 in 3T3-L1 pre-adipocytes and

doi:10.6342/NTU201901578

adipocytes

To monitor the intra-cellular localization of endogenous S14 during 3T3-L1 differentiation, we used immunofluorescence staining to detect S14 in 3T3-L1 pre-adipocytes and adipocytes. We found that S14 is mainly localized in the nucleus in pre-adipocyte, but mainly localized in the cytoplasm associated with lipid droplets in differentiated adipocytes (Figure 9). These experiments imply that S14 may play different roles in pre-adipocytes and adipocytes, and may be a protein with dual functions.

3.2.6 S14 activates KLF15 and PPARγ2 promoter activity in adipocytes

Both KLF15 and PPARγ2 are two important transcription activators for adipogenesis (Berger, 2005; Mori et al., 2005; Siersbaek et al., 2010; Wu and Wang, 2013). The expression of both transcription factors was down-regulated by S14 knockdown in 3T3-L1 (Figure 8c). To investigate how S14 altered the transcription activity of KLF15 and PPARγ2, we constructed approximately 2-kb KLF15 and PPARγ2 promoters to drive the expression of luciferase gene. Co-transfection of a construct over-expressing *S14* gene with the promoter construct of these two genes in 3T3-L1 pre-adipocytes and adipocytes were performed to investigate if S14 can activate these promoters or not. S14 only slightly increased the promoter activity of KLF15, but not PPARγ2 in pre-adipocytes (Figure 10a). The promoter activity of KLF15 and PPARγ2 both were increased by co-transfection of S14 construct in differentiated adipocytes (1.81 and 1.41-folds) (Figure 10b). Next, we generated promoter deletion constructs of KLF15 to map the specific response elements. No matter what promoter deletion constructs were used, the promoter activity was increased in pre-adipocyte by S14 co-transfection (Figure 10c).

In addition, we performed chromatin immunoprecipitation (ChIP) assay with S14

doi:10.6342/NTU201901578

antibody to investigate the possible DNA sequences that may interact with S14 protein. Figure 11a showed that the ChIP was working. We also demonstrated that the S14 protein existed in the chromatin sample section by Western blot (Figure 11b). We sent the final samples to Next Generation Gene Sequencing and Bioinformatics Analysis Services Center of National Taiwan University Hospital. The analysis is still in progress.

3.2.7 Analysis of the potential interacting protein of S14 by IP-Mass

Previous studies showed that S14 was translocated into nucleus upon T3 treatment and interacted with thyroid hormone receptor in breast cancer cell line, suggesting that S14 may act as a transcription factor (Chou et al., 2007). However, there was no reported nuclear localization signal (NLS) or nuclear export signal (NES) in the S14 sequence. We speculated that S14 might regulate signal pathways of adipogenesis through interact with other proteins. To demonstrate the possibility, we treated 3T3-L1 pre-adipocytes with formaldehyde to cross-link proteins and then performed immunoprecipitation experiments to pull-down endogenous S14. However, there was no detectable S14 by Western blot. Next, we tried to use the overexpressed tagged-S14 in pre-adipocytes then performed the same experiments. However, 3T3-L1 cells were very difficult to transfect. Then we turned to 293T cell line as the model. We overexpressed pcDNA3.1-S14-Flag into HEK293T cells and pull down the overexpressed tagged-S14 by immunoprecipitation and run the SDS-PAGE. We separated the gels for mass spectrometry analysis to identify the interacting proteins. Comparing the vector control, we found several potential interacting proteins, such as ZA2G, GCN2, APOD and KLF7 (Table 12).

3.2.8 Cytokines and ER stress down-regulated S14 mRNA Expression

PPARγ2 is the master gene for adipogenesis as well as the key regulator of insulin

doi:10.6342/NTU201901578

sensitivity. Since S14 may regulate the expression of PPARγ2, we postulated that some biological factors which modulate insulin sensitivity, such as inflammatory cytokines and ER stress may regulate Spot 14 expression. The Spot 14 mRNA expression levels were measured in the differentiated 3T3-L1 adipocytes treated with inflammatory, cytokines IL-1β and TNF-α, and ER stress inducers, tunicamycin and thapsigargin. Its mRNA expression levels were reduced to 10%, 12%, 20% and less than 10% of the controls, respectively by IL-1β, TNF-α, tunicamycin (TUN) and thapsigargin (TSG) treatment (Figure 12b). Likewise, the mRNA levels of adiponectin, a biomarker of insulin sensitivity of the adipose tissues (Lu et al., 2008), were significantly down-regulated respectively by 55%, 44%, 66% and more than 90% with the same treatment (Figure 12a). In contrast, the mRNA of S14R was slightly altered by the treatment of IL-1β, TNF-α, TUN and TSG (Figure 12c). These results suggest that S14 may participate in the pathophysiology of obesity-related insulin resistance induced by inflammation and ER stress (Figure 12b).

We further tested whether signaling proteins such as Jak2, p44/42 MAP kinase, p38 MAP kinase, and PI3-kinase, which have been implicated in cytokine or ER stress signaling, might play a role in downregulation of adiponectin and S14 gene expression. For this purpose, 3T3-L1 adipocytes were pretreated with specific pharmacological inhibitors for 1 hour before cytokines or ER stress inducers were added for 24 hours.

IMD-0345, an IKK-β inhibitor, inhibits the phosphorylation of IκB and the nuclear translocation of NFκB (Kamon et al., 2004). It has been shown to restore TNFα-mediated downregulation of adiponectin secretion in 3T3-L1 adipocytes (Hino and Nagata, 2012; Kamon et al., 2004). In our study, we found that IMD-0354 can restore IL1-β, TUN and TSG-mediated S14 downregulation by 16-, 5.4-, and 12.3-folds respectively (Figure 13). The mRNA expression of ADQ also was recovered in

doi:10.6342/NTU201901578

adipocytes with IL-1β or TUN by IMD-0354 treatment, but there was no difference from TSG treatment with IMD-0354 in adipocytes (Figure 13). The reduction of mRNA expressions of S14 and ADQ of adipocytes by IL-1β, TUN or TSG did not change with another IKKβ inhibitor, SC-514, treatment. On the other hand, LY294002, a chemical inhibitor of phosphatidylinositol 3-kinase (PI3K), also restored IL1-β, TUN and TSG-mediated S14 downregulation (10.8, 14.4, and 11.6-folds respectively) (Figure 13). The mRNA expressions of ADQ were partially restored, too. Previous studies have shown that PI3K plays an important role in terminal differentiation of 3T3-L1 pre-adipocyte cells into adipocytes (Xia and Serrero, 1999). The inhibition of PI3K by a chemical inhibitor LY294002 blocked insulin-induced lipid accumulation in 3T3-L1 cells (Xia and Serrero, 1999). We also found that only ER stress-mediated S14 and ADQ downregulation could be recovered by U0126 treatment, which is a specific inhibitor of ERK activity. Specific MAPK inhibitors such as MEK-1 inhibitor PD98059, p38 MAPK inhibitor SB203580, and JNK inhibitor SP 600125 were also used, but there was no change of the mRNA expressions of S14 and ADQ. These results suggested that IL-1β, the ER stress inducers, TUN and TSG, may regulate S14 mRNA expression through NF-κB, PI3k and ERK signaling.

3.3 Animal model

Previous studies showed that S14 knockout mice had better resistance to diet-induced obesity and better glucose tolerance comparing to wild types. However, the exact role of S14 in the adipose tissue has not been well investigated. Therefore, we try to establish adipose tissue-specific conditional S14 knockout mice to investigate the role of S14 in adipose tissue in animal model. We performed genotyping by genomic DNA sequencing to confirm the orientations of the inserted sequences (Figure 14a). Next, we breed this

doi:10.6342/NTU201901578

C57BL/6J-Thrsp-loxp strain mice with C57BL/6-Adipoq-cre mice which was purchased from National Laboratory Animal Center to generate the adipose tissue-specific S14 conditional knockout mice (Figure 14b). After intraperitoneal injection of tamoxifen, the DNA rearrangement patterns of S14 in mice liver and adipose tissue were analyzed (Figure 14c). However the result of genetic alteration was not as expected. This is still under investigation.

doi:10.6342/NTU201901578

Chapter 4. Discussion and future perspectives

We successfully developed a competitive ELISA system to measure serum S14 levels in human subjects and applied this method in the analysis of human diseases. We also performed several *in vitro* cellular experiments to investigate the molecular mechanism regarding the role of S14 in adipogenesis.

4.1 S14 and thyroid hormone

Thyroid dysfunction may affect adipocyte function and lipid metabolism (Rizos et al., 2011). Patients with hyperthyroidism usually have decreased levels of lipid (Pontikides and Krassas, 2007), but increased concentrations of plasma fatty acids (Silva, 2003). Thyroid hormones are a well-known inducer of hepatic *de novo* lipogenesis (Sinha et al., 2018). Previous studies demonstrated that thyroid hormone can upregulate S14 gene expression in the liver of thyroidectiomized rat (Franklyn et al., 1989; Seelig et al., 1981). In addition, S14 play a role in hepatic fatty acid synthesis of rat (Kinlaw et al., 1995; Zhu et al., 2005). We used our home-made ELISA system to measure serum S14 levels in human subjects and evaluated the effect of thyroid function status on serum S14 level. We found that patients with hyperthyroidism had significantly higher serum S14 levels than subjects with euthyroidism. This observation is consistent with previous animal experiments (Seelig et al., 1981). We suppose that liver might at least be one of the main sources of the increased serum S14 (Figure 15a) of hyperthyroidism group. However, the exact mechanism remains to be explored.

4.2 S14 and metabolic syndrome

A chronic state of inflammation appears to be the central mechanism underlying the pathophysiology of insulin resistance and MetS (Kahn and Flier, 2000). To investigate the mechanism, we treated 3T3-L1 adipocyte with IL-1β to establish a cell model to

doi:10.6342/NTU201901578

mimic cytokines-induced insulin resistance. We performed gene microarray for analyzing the gene expression differences between 3T3-L1 adipocytes which were treated with and without IL-1β. S14 was the most significantly down-regulated gene in IL-1β treated cells compared with the controls. Previous studies have shown that S14 mRNA expression in the adipose tissue of obese subjects was lower than non-obese individuals (Kirschner and Mariash, 1999). Compared to wild type animals, the *Thrsp* null mouse fat mass was significantly reduced and had better glucose tolerance (Anderson et al., 2009). In our study, we found that the subjects with high body fat or BMI, metabolic syndrome, central obesity, high TG and low HDL-C had significantly lower serum S14 levels than the people without. On the other hand, we knockdown S14 with shRNA in 3T3-L1 pre-adipocyte and we found that the lipid droplets accumulation were significantly decreased than control group. These results imply S14 might play a role of adipogenesis in adipocyte differentiation and the pathology of inflammatory-related insulin resistance. We proposed that the mechanism of reduced serum S14 level in human metabolic syndrome is similar to the case of adiponectin. Adiponectin is a protein hormone which plays an important role in many metabolic processes, such as regulating glucose levels and fatty acid oxidation (Lu et al., 2008). Many studies have found that adiponectin inversely correlated with BMI, BW, or hypertriglyceridemia in patient populations (Falasca et al., 2006; Gomez Rosso et al., 2009; Yang et al., 2002). When BW is reduced, insulin sensitivity is improved and the serum levels of adiponectin increased (Yang et al., 2001). However, the exact mechanism remains to be explored. We propose that the decreased serum S14 levels in MetS subjects were due to reduce S14 gene expression in the adipose tissue (Figure 15b).

doi:10.6342/NTU201901578

4.3 S14 and liver function

S14 has been reported to be expressed in liver (Jump and Oppenheimer, 1985) and S14 may play a role in the pathogenesis of NAFLD (Wu et al., 2013). However, there is no direct evidence supporting the impact of S14 expression level on liver function in human yet. In our study, patients with hyperthyroidism had higher serum AST and ALT levels than the subjects with euthyroidism. On the other hand, subjects with MetS had higher ALT levels than the subjects without MetS. However, there was no association between serum level of logS14 with AST or ALT. In the future, we plan to collect patients with NAFLD for further analysis to directly explore this issue.

4.4 S14 and age

Our two clinical studies both revealed a borderline negative association of age with logS14. Before our studies, there is no human study showing the S14 mRNA or protein expression levels with age. Jump DB and Oppenheimer JH reported that with the age increasing from one to ten months, the rat S14 mRNA expression levels increased about 4.48 fold in the liver, but reduced nearly 50% in the epididymal fat (Jump and Oppenheimer, 1985). They did not investigate the detailed mechanism. However, previous studies have demonstrated that aging would affect the regulation of lipogenesis in humans and rats (Kamel et al., 2004). Dr. Kamel and his colleagues measured the basal and insulin-induced lipogenesis from the adipose tissues of infants (mean 1.5 months), children (mean 4 years old), and adult humans (mean 31 years old), and male weaned (4 weeks) and male young adult (9 weeks) Fischer rats by determining the incorporation of glucose into lipids (Kamel et al., 2004). They observed that the basal, insulin-induced and total lipogenesis were all higher in infants than in children and adults (Kamel et al., 2004). They also found that basal and insulin-induced lipogenesis

doi:10.6342/NTU201901578

in adipocytes were higher from weaned than adult rats (Kamel et al., 2004). These results indicate that age-dependent regulation of adipocyte lipogenesis (Kamel et al., 2004). Whether the expression pattern of S14 also related to aging remains further investigation.

4.5 S14 and gender

In our study, we found that female gender had higher serum S14 levels than male subjects. In univariate regression model with logS14 as dependent variable, the associations between logS14 and many independent variables, such as BW and BMI, were prominent in females but not in males. The fat distribution is different in adult men and women (Karastergiou et al., 2012). Several sex hormones such as progesterone, estrogens, and androgens have been reported to involve in the regulation of adipose tissue metabolism (Duan et al., 2013; Ren et al., 2017; Stelmanska and Swierczynski, 2013). We propose that the difference of the correlations between S14 and BW or BMI in different gender might due to the effect of sex hormones in body.

In 2012, Ewa Stelmanska and Julian Swierczynski analyzed the lipogenic enzyme mRNA expressions in inguinal adipose tissue of rats with or without progesterone treatment (Stelmanska and Swierczynski, 2013). They found that the expression level of S14 mRNA in female rats was increased with progesterone administration, but there was no effect in male rats (Stelmanska and Swierczynski, 2013). In addition, chicken *THRSP* gene expression in the liver was significantly upregulated when chickens were treated with 17β-estradiol through an estrogen receptor binding site located in the *THRSP* promoter (Ren et al., 2017). On the other hand, Jinlin Duan and her colleagues used Affymetrix microarray technology to analyze the gene expression profiles of livers from capons and intact male chickens for investigating the influence of male hormone,

doi:10.6342/NTU201901578

androgen, on fat accumulation in the chicken (Duan et al., 2013). Capons, male chickens whose testes have been surgically incised, show a significant increase in fat accumulation compared to intact male chickens. They found that compared to intact male chickens, the genes of hepatic lipogenic biosynthesis of capons were highly enriched, including *THRSP* gene, expression which was upregulated by 2.2-fold in the liver (Duan et al., 2013). These results suggest that sex hormones might involve in regulating the expression of S14 and might contribute to the gender difference of S14 levels in humans in our studies. Whether this is true awaits further investigation.

4.6 S14 and gene regulation

In the past decades, how adipogenesis is regulated at the transcriptional level is extensively studied (Ali et al., 2013; Wu and Wang, 2013). In this study, we found that S14 mRNA increased dramatically during 3T3-L1 differentiation. After knocking down S14 mRNA expression by lentiviral transduction in 3T3-L1 pre-adipocyte, the differentiation was deterred and many adipocyte differentiation related gene were affected. In contrast, S14R not only was not robustly activated during adipocyte differentiation but also was unable to complement the loss of S14. In addition, we found that S14 was localized in different location of different cell status. S14 was mainly localized in the nucleus in pre-adipocyte, but was mainly localized in the cytoplasm associated with lipid droplets in differentiated adipocytes. These observations suggest that S14 plays an important role in lipid accumulation in the adipose tissue and may have dual function in different stages of adipocyte differentiation. We also speculate that S14 may be a regulator for the transcriptional cascade of adipogenesis. Some protein, such as p53, has been reported to shuttle between the nucleus and the cytoplasm in a cell-cycle specific manner through its nuclear localization signal (NLS) or binding with

doi:10.6342/NTU201901578

other proteins and play different roles (O'Brate and Giannakakou, 2003). However, there was no reported NLS or nuclear export signal (NES) in the S14 sequence. Many questions deserve further investigation, including what are the functions for S14 at different localizations, and in different differentiation stage, how S14 regulates gene expressions in nucleus, and how S14 shuttles between nucleus and cytoplasm. We propose that S14 might regulate signal pathways of adipogenesis through interactions with other proteins. By IP-MASS analysis, we found several potential interacting proteins, such as ZA2G, GCN2, APOD and KLF7 were expressed in the S14 construct transfected cell lines but not in the control group. All these potential interacting proteins have been reported to play roles in lipid metabolism or related pathways. ZA2G, also called AZGP1 (Alpha-2-Glycoprotein 1), acts as a lipid mobilizing factor to induce lipolysis in adipocytes and plays an important role in lipid utilization and loss of adipose tissue (Bao et al., 2005). GCN2 encodes a member of a kinases family that phosphorylates the alpha subunit of eukaryotic translation initiation factor-2 (ElF2) and plays a key role in modulating amino acid metabolism in yeast and mammals (Guo and Cavener, 2007). APOD (Apolipoprotein D), a lipid carrier protein, was markedly responsive to liver X receptor (LXR) expression and involved in modulating lipid metabolism in adipocytes (Hummasti et al., 2004). Because the experiments were performed in 293T cell, not in 3T3-L1 cell line, whether S14 really regulates the signal pathways of adipogenesis through interacting with these proteins remains to be confirmed.

4.7 The limitations in these two clinical studies

There were several limitations in our clinical studies. First, they were cross-sectional studies. We cannot determine the causality between serum S14 levels and the metabolic

doi:10.6342/NTU201901578

abnormalities, but we speculate that reduced S14 expression is the result of the metabolic abnormality. On the other hand, our case numbers of the hyperthyroidism study were small. Nevertheless, we still saw a significant relation between thyroid function and serum S14 levels. More subjects should be recruited in the future. Second, the S14 paralogous protein (S14R) is 32% homologous to S14 in amino acid sequences (Colbert et al., 2010). The antibody used in our immunoassay was polyclonal. The antibody may cross react with S14R in our ELISA. However, S14R was known not to be influenced by thyroid hormone treatment (Aipoalani et al., 2010) and the mRNA expression level of S14R was demonstrated to be far lower than S14 in the adipose tissues (about 1:100) (Harvatine and Bauman, 2006). We believe that the use of our S14 immunoassay is reliable in our studies. But specific antibodies to S14 should be generated in the future to solve this problem. Lastly, we did not have sufficient biochemical data such as insulin levels or free T3 levels to directly address the relationship between S14 and insulin resistance or thyroid function.

4.8 Future perspectives

Adipose tissue is one of the primary sites of S14 gene expression. Deletion of S14 resulted in resistance to diet-induced obesity and improvement in insulin sensitivity as well as glucose tolerance in mice model (Anderson et al., 2009). In obese individuals, S14 mRNA expression is down-regulated comparing to healthy controls (Kirschner and Mariash, 1999). In response to fasting, the S14 mRNA expression in the adipose tissues was suppressed in the healthy controls, but not in the obese subjects (Kirschner and Mariash, 1999). These evidences suggest that S14 may play a significant role in regulating fatty acid synthesis, in the pathogenesis of obesity, and obesity-related co-morbidities in humans (Kirschner and Mariash, 1999; Ortega et al., 2010). However,

doi:10.6342/NTU201901578

since S14 is rarely studied in adipose tissue, and we found that S14 knockdown seriously affects the differentiation ability of adipocytes in 3T3-L1. Two groups ever try to establish *S14* knockout model *in vivo* to demonstrate the issue (LaFave et al., 2006). One group deleted the proximal promoter and entire coding sequence of *S14* gene. However, they found the homozygous mutation of this model was early embryonic lethal. Dr. Cary N. Mariash and his colleagues deleted all expect the first 21 amino acids of the *S14* gene. The *S14* knockout offspring was normal. Northern analysis and Western blotting shown there was no S14 mRNA and protein expressions in the knockout mice liver and mammary gland (LaFave et al., 2006). The authors suggested that the 21 amino acids may code for a small peptide that supplies the same essential function as S14 in the embryo (LaFave et al., 2006). The S14 null mice exhibit resistance to diet-induced obesity and improved glucose and insulin tolerance (Anderson et al., 2009). However the lack of S14 in different tissues may have varying phenotypic effects. The level of lipogenesis decreased in the lactating mammary gland, whereas hepatic lipogenesis did not (Zhu et al., 2005; Zhu et al., 2001). They suggested that S14R, the paralog of S14, compensated the function of S14 in hepatic lipogenesis. In order to specifically investigate the role of S14 in adipose tissue; we established a strain of conditional adipose-specific S14 knockout mice. We hope this strain will help us to learn more about the actual function of S14 in fat synthesis, the pathophysiological mechanisms of metabolic syndrome, and to develop treatment in the future.

S14 may play a role in the pathogenesis of NAFLD (Wu et al., 2013). We want to establish a strain of liver-specific conditional S14 knockout mice to study the role of S14 in hepatic lipogenesis and the physiological mechanisms of fatty liver in the future. Plasma serine protease proprotein convertase subtilisin-kexin type 9 (PCSK9) enhanced the degradation of LDL receptor, resulting in accumulation of LDL-C in the circulation

doi:10.6342/NTU201901578

(Nishikido and Ray, 2018). Inclisiran, a chemically synthesized small interfering RNAs (siRNAs), administration in human is a new therapeutic strategy for hypercholesterolemia (Nishikido and Ray, 2018). Inclisiran can inhibit translation of PCSK9 mRNA and turn off PCSK9 production then the circulating LDL-C can be reduced (Nishikido and Ray, 2018). If we can clarify the role of S14 in hepatic lipogenesis in animal model, S14 may also be a therapeutic target for hypertriglyceridemia in the future.

We also want to use our home-made S14 ELISA to measure serum S14 and other endocrine and metabolic diseases, such as obesity, T2DM, NAFLD, hypertriglyceridemia and so on.

doi:10.6342/NTU201901578

Appendix

References

Adamczak M, Wiecek A. The Adipose Tissue as an Endocrine Organ. Seminars in Nephrology. 2013 Jan;33(1):2-13.

Aipoalani DL, O'Callaghan BL, Mashek DG, Mariash CN, Towle HC. Overlapping roles of the glucose-responsive genes, S14 and S14R, in hepatic lipogenesis. Endocrinology. 2010 May;151(5):2071-7.

Al-Shoumer KA, Vasanthy BA, Al-Zaid MM. Effects of treatment of hyperthyroidism on glucose homeostasis, insulin secretion, and markers of bone turnover. Endocr Pract. 2006 Mar-Apr;12(2):121-30.

Alberti KG, Zimmet P, Shaw J, Group IDFETFC. The metabolic syndrome--a new worldwide definition. Lancet. 2005 Sep 24-30;366(9491):1059-62.

Alberti KG, Zimmet PZ. Definition, diagnosis and classification of diabetes mellitus and its complications. Part 1: diagnosis and classification of diabetes mellitus provisional report of a WHO consultation. Diabet Med. 1998 Jul;15(7):539-53.

Ali AT, Hochfeld WE, Myburgh R, Pepper MS. Adipocyte and adipogenesis. Eur J Cell Biol. 2013 Jun-Jul;92(6-7):229-36.

Ameer F, Scandiuzzi L, Hasnain S, Kalbacher H, Zaidi N. De novo lipogenesis in health and disease. Metabolism. 2014 Jul;63(7):895-902.

Anderson GW, Zhu Q, Metkowski J, Stack MJ, Gopinath S, Mariash CN. The Thrsp null mouse (Thrsp(tm1cnm)) and diet-induced obesity. Mol Cell Endocrinol. 2009 Apr 10;302(1):99-107.

Bao Y, Bing C, Hunter L, Jenkins JR, Wabitsch M, Trayhurn P. Zinc-alpha2-glycoprotein, a lipid mobilizing factor, is expressed and secreted by human (SGBS) adipocytes. FEBS Lett. 2005 Jan 3;579(1):41-7.

doi:10.6342/NTU201901578

Berger JP. Role of PPARgamma, transcriptional cofactors, and adiponectin in the regulation of nutrient metabolism, adipogenesis and insulin action: view from the chair. Int J Obes (Lond). 2005 Mar;29 Suppl 1(S3-4.

Berti C, Fontanella B, Ferrentino R, Meroni G. Mig12, a novel Opitz syndrome gene product partner, is expressed in the embryonic ventral midline and co-operates with Mid1 to bundle and stabilize microtubules. BMC Cell Biol. 2004 Feb 29;5(9.

Biondi B. How could we improve the increased cardiovascular mortality in patients with overt and subclinical hyperthyroidism? Eur J Endocrinol. 2012 Sep;167(3):295-9.

Blennemann B, Leahy P, Kim TS, Freake HC. Tissue-specific regulation of lipogenic mRNAs by thyroid hormone. Mol Cell Endocrinol. 1995 Apr 28;110(1-2):1-8.

Braverman LE. Various aspects of thyroid physiology and pathology contributed by international experts. Curr Opin Endocrinol Diabetes Obes. 2012 Oct;19(5):381.

Campbell M, Jialal I. Physiology, Endocrine Hormones. StatPearls. 2019

Canaris GJ, Manowitz NR, Mayor G, Ridgway EC. The Colorado thyroid disease prevalence study. Arch Intern Med. 2000 Feb 28;160(4):526-34.

Carling T, Udelsman R. Thyroid cancer. Annu Rev Med. 2014 65(125-37.

Chen YT, Tseng FY, Chen PL, Chi YC, Han DS, Yang WS. Serum Spot 14 concentration is negatively associated with thyroid-stimulating hormone level. Medicine (Baltimore). 2016 Oct;95(40):e5036.

Chen YT, Tseng PH, Tseng FY, Chi YC, Han DS, Yang WS. The serum level of a novel lipogenic protein Spot 14 was reduced in metabolic syndrome. PLoS One. 2019 14(2):e0212341.

Chou WY, Cheng YS, Ho CL, Liu ST, Liu PY, Kuo CC, Chang HP, Chen YH, Chang

doi:10.6342/NTU201901578

GG, Huang SM. Human spot 14 protein interacts physically and functionally with the thyroid receptor. Biochem Biophys Res Commun. 2007 May 25;357(1):133-8.

Christodoulides C, Vidal-Puig A. PPARs and adipocyte function. Mol Cell Endocrinol. 2010 Apr 29;318(1-2):61-8.

Chrousos GP, Gold PW. The concepts of stress and stress system disorders. Overview of physical and behavioral homeostasis. JAMA. 1992 Mar 4;267(9):1244-52.

Clement J, Hausdorf S, Keck FS, Loos U. Thyroid hormones alter mRNA activity profiles of differentiated 3T3-L1-cells. Horm Metab Res Suppl. 1987 17(23-5.

Coelho M, Oliveira T, Fernandes R. Biochemistry of adipose tissue: an endocrine organ. Archives of Medical Science. 2013 Apr;9(2):191-200.

Colbert CL, Kim CW, Moon YA, Henry L, Palnitkar M, McKean WB, Fitzgerald K, Deisenhofer J, Horton JD, Kwon HJ. Crystal structure of Spot 14, a modulator of fatty acid synthesis. Proc Natl Acad Sci U S A. 2010 Nov 2;107(44):18820-5.

Danzi S, Klein I. Thyroid hormone and the cardiovascular system. Med Clin North Am. 2012 Mar;96(2):257-68.

Darlington GJ, Ross SE, MacDougald OA. The role of C/EBP genes in adipocyte differentiation. J Biol Chem. 1998 Nov 13;273(46):30057-60.

Davidson JM, Chen JJ, Crapo L, Gray GD, Greenleaf WJ, Catania JA. Hormonal changes and sexual function in aging men. J Clin Endocrinol Metab. 1983 Jul;57(1):71-7.

Duan J, Shao F, Shao Y, Li J, Ling Y, Teng K, Li H, Wu C. Androgen inhibits abdominal fat accumulation and negatively regulates the PCK1 gene in male chickens. PLoS One. 2013 8(3):e59636.

Expert Panel on Detection E, Treatment of High Blood Cholesterol in A. Executive

doi:10.6342/NTU201901578

Summary of The Third Report of The National Cholesterol Education Program (NCEP) Expert Panel on Detection, Evaluation, And Treatment of High Blood Cholesterol In Adults (Adult Treatment Panel III). JAMA. 2001 May 16;285(19):2486-97.

Falasca K, Manigrasso MR, Racciatti D, Zingariello P, Dalessandro M, Ucciferri C, Mancino P, Marinopiccoli M, Petrarca C, Conti P, et al. Associations between hypertriglyceridemia and serum ghrelin, adiponectin, and IL-18 levels in HIV-infected patients. Ann Clin Lab Sci. 2006 Winter;36(1):59-66.

Flamment M, Hajduch E, Ferre P, Foufelle F. New insights into ER stress-induced insulin resistance. Trends Endocrinol Metab. 2012 Aug;23(8):381-90.

Franklyn JA, King S, Ahlquist JA, Sheppard MC. Effect of hypothyroidism and thyroid hormone treatment of the rat on hepatic Spot 14 and thyroxine binding prealbumin mRNAs. Acta Endocrinol (Copenh). 1989 Sep;121(3):383-8.

Frayn KN. Adipose tissue and the insulin resistance syndrome. Proc Nutr Soc. 2001 Aug;60(3):375-80.

Freake HC, Moon YK. Hormonal and nutritional regulation of lipogenic enzyme mRNA levels in rat primary white and brown adipocytes. J Nutr Sci Vitaminol (Tokyo). 2003 Feb;49(1):40-6.

Freake HC, Oppenheimer JH. Stimulation of S14 mRNA and lipogenesis in brown fat by hypothyroidism, cold exposure, and cafeteria feeding: evidence supporting a general role for S14 in lipogenesis and lipogenesis in the maintenance of thermogenesis. Proc Natl Acad Sci U S A. 1987 May;84(9):3070-4.

Gomez Rosso L, Merono T, Benitez MB, Lopez G, Giunta G, D'Ambrosio ML, Wikinski R, Cuniberti L, Brites F. Low adiponectin levels in primary hypertriglyceridemic male patients. Nutr Metab Cardiovasc Dis. 2009

doi:10.6342/NTU201901578

Feb;19(2):135-9.

Green H, Meuth M. An established pre-adipose cell line and its differentiation in culture. Cell. 1974 Oct;3(2):127-33.

Gregoire FM, Smas CM, Sul HS. Understanding adipocyte differentiation. Physiol Rev. 1998 Jul;78(3):783-809.

Grimaldi PA. The roles of PPARs in adipocyte differentiation. Prog Lipid Res. 2001 Jul;40(4):269-81.

Grundy SM, Cleeman JI, Daniels SR, Donato KA, Eckel RH, Franklin BA, Gordon DJ, Krauss RM, Savage PJ, Smith SC, Jr., et al. Diagnosis and management of the metabolic syndrome: an American Heart Association/National Heart, Lung, and Blood Institute Scientific Statement. Circulation. 2005 Oct 25;112(17):2735-52.

Guo F, Cavener DR. The GCN2 eIF2alpha kinase regulates fatty-acid homeostasis in the liver during deprivation of an essential amino acid. Cell Metab. 2007 Feb;5(2):103-14.

Hardy OT, Czech MP, Corvera S. What causes the insulin resistance underlying obesity? Curr Opin Endocrinol Diabetes Obes. 2012 Apr;19(2):81-7.

Harvatine KJ, Bauman DE. SREBP1 and thyroid hormone responsive spot 14 (S14) are involved in the regulation of bovine mammary lipid synthesis during diet-induced milk fat depression and treatment with CLA. J Nutr. 2006 Oct;136(10):2468-74.

Hausdorf S, Clement J, Loos U. Expression of S14 gene during differentiation of 3T3-L1-cells. Horm Metab Res. 1988 Nov;20(11):723-4.

Hino K, Nagata H. Screening for adiponectin secretion regulators. Vitam Horm. 2012 90(125-41.

Hirsch PF, Lester GE, Talmage RV. Calcitonin, an enigmatic hormone: does it have a

doi:10.6342/NTU201901578

function? J Musculoskelet Neuronal Interact. 2001 Jun;1(4):299-305.

Hummasti S, Laffitte BA, Watson MA, Galardi C, Chao LC, Ramamurthy L, Moore JT, Tontonoz P. Liver X receptors are regulators of adipocyte gene expression but not differentiation: identification of apoD as a direct target. J Lipid Res. 2004 Apr;45(4):616-25.

Hung CS, Tseng PH, Tu CH, Chen CC, Liao WC, Lee YC, Chiu HM, Lin HJ, Ho YL, Yang WS, et al. Nonalcoholic Fatty Liver Disease Is Associated With QT Prolongation in the General Population. J Am Heart Assoc. 2015 Jul 21;4(7)

Hung CS, Tseng PH, Tu CH, Chen CC, Liao WC, Lee YC, Chiu HM, Lin HJ, Yang WS, Chen MF, et al. Increased Pancreatic Echogenicity with US: Relationship to Glycemic Progression and Incident Diabetes. Radiology. 2018 Jun;287(3):853-63.

Hwang LC, Bai CH, Chen CJ. Prevalence of obesity and metabolic syndrome in Taiwan. J Formos Med Assoc. 2006 Aug;105(8):626-35.

Jump DB, Narayan P, Towle H, Oppenheimer JH. Rapid effects of triiodothyronine on hepatic gene expression. Hybridization analysis of tissue-specific triiodothyronine regulation of mRNAS14. J Biol Chem. 1984 Mar 10;259(5):2789-97.

Jump DB, Oppenheimer JH. High basal expression and 3,5,3'-triiodothyronine regulation of messenger ribonucleic acid S14 in lipogenic tissues. Endocrinology. 1985 Dec;117(6):2259-66.

Kahn BB, Flier JS. Obesity and insulin resistance. J Clin Invest. 2000 Aug;106(4):473-81.

Kamel AF, Norgren S, Strigard K, Thorne A, Fakhrai-Rad H, Galli J, Marcus C. Age-dependent regulation of lipogenesis in human and rat adipocytes. J Clin

doi:10.6342/NTU201901578

Endocrinol Metab. 2004 Sep;89(9):4601-6.

Kamon J, Yamauchi T, Muto S, Takekawa S, Ito Y, Hada Y, Ogawa W, Itai A, Kasuga M, Tobe K, et al. A novel IKKbeta inhibitor stimulates adiponectin levels and ameliorates obesity-linked insulin resistance. Biochem Biophys Res Commun. 2004 Oct 8;323(1):242-8.

Karastergiou K, Smith SR, Greenberg AS, Fried SK. Sex differences in human adipose tissues - the biology of pear shape. Biol Sex Differ. 2012 May 31;3(1):13.

Kaur J. A comprehensive review on metabolic syndrome. Cardiol Res Pract. 2014 2014(943162.

Kim CW, Moon YA, Park SW, Cheng D, Kwon HJ, Horton JD. Induced polymerization of mammalian acetyl-CoA carboxylase by MIG12 provides a tertiary level of regulation of fatty acid synthesis. Proc Natl Acad Sci U S A. 2010 May 25;107(21):9626-31.

Kinlaw WB, Church JL, Harmon J, Mariash CN. Direct evidence for a role of the "spot 14" protein in the regulation of lipid synthesis. J Biol Chem. 1995 Jul 14;270(28):16615-8.

Kirschner LS, Mariash CN. Adipose S14 mRNA is abnormally regulated in obese subjects. Thyroid. 1999 Feb;9(2):143-8.

Knudsen N, Laurberg P, Rasmussen LB, Bulow I, Perrild H, Ovesen L, Jorgensen T. Small differences in thyroid function may be important for body mass index and the occurrence of obesity in the population. J Clin Endocrinol Metab. 2005 Jul;90(7):4019-24.

LaFave LT, Augustin LB, Mariash CN. S14: insights from knockout mice. Endocrinology. 2006 Sep;147(9):4044-7.

Lane MD, Tang QQ, Jiang MS. Role of the CCAAT enhancer binding proteins (C/EBPs)

doi:10.6342/NTU201901578

in adipocyte differentiation. Biochem Biophys Res Commun. 1999 Dec 29;266(3):677-83.

Li L, Wang C, Bao Y, Peng L, Gu H, Jia W. Optimal body fat percentage cut-offs for obesity in Chinese adults. Clin Exp Pharmacol Physiol. 2012 Apr;39(4):393-8.

Lu JY, Huang KC, Chang LC, Huang YS, Chi YC, Su TC, Chen CL, Yang WS. Adiponectin: a biomarker of obesity-induced insulin resistance in adipose tissue and beyond. J Biomed Sci. 2008 Sep;15(5):565-76.

Maratou E, Hadjidakis DJ, Peppa M, Alevizaki M, Tsegka K, Lambadiari V, Mitrou P, Boutati E, Kollias A, Economopoulos T, et al. Studies of insulin resistance in patients with clinical and subclinical hyperthyroidism. Eur J Endocrinol. 2010 Oct;163(4):625-30.

Minteer D, Marra KG, Rubin JP. Adipose-derived mesenchymal stem cells: biology and potential applications. Adv Biochem Eng Biotechnol. 2013 129(59-71.

Mollard P, Schaeffer M. Imaging endocrinology in animal models of endocrine disease. Best Pract Res Clin Endocrinol Metab. 2018 Jun;32(3):317-28.

Mori T, Sakaue H, Iguchi H, Gomi H, Okada Y, Takashima Y, Nakamura K, Nakamura T, Yamauchi T, Kubota N, et al. Role of Kruppel-like factor 15 (KLF15) in transcriptional regulation of adipogenesis. J Biol Chem. 2005 Apr 1;280(13):12867-75.

Nishikido T, Ray KK. Inclisiran for the treatment of dyslipidemia. Expert Opin Investig Drugs. 2018 Mar;27(3):287-94.

O'Brate A, Giannakakou P. The importance of p53 location: nuclear or cytoplasmic zip code? Drug Resist Updat. 2003 Dec;6(6):313-22.

Ortega FJ, Vazquez-Martin A, Moreno-Navarrete JM, Bassols J, Rodriguez-Hermosa J, Girones J, Ricart W, Peral B, Tinahones FJ, Fruhbeck G, et al. Thyroid hormone

doi:10.6342/NTU201901578

responsive Spot 14 increases during differentiation of human adipocytes and its expression is down-regulated in obese subjects. Int J Obes (Lond). 2010 Mar;34(3):487-99.

Park S, Hwang IW, Makishima Y, Perales-Clemente E, Kato T, Niederlander NJ, Park EY, Terzic A. Spot14/Mig12 heterocomplex sequesters polymerization and restrains catalytic function of human acetyl-CoA carboxylase 2. J Mol Recognit. 2013 Dec;26(12):679-88.

Perez-Castillo A, Hernandez A, Pipaon C, Santos A, Obregon MJ. Multiple regulation of S14 gene expression during brown fat differentiation. Endocrinology. 1993 Aug;133(2):545-52.

Pirahanchi Y, Jialal I. Physiology, Thyroid Stimulating Hormone (TSH). StatPearls. 2019

Pontikides N, Krassas GE. Basic endocrine products of adipose tissue in states of thyroid dysfunction. Thyroid. 2007 May;17(5):421-31.

Ranganathan G, Unal R, Pokrovskaya I, Yao-Borengasser A, Phanavanh B, Lecka-Czernik B, Rasouli N, Kern PA. The lipogenic enzymes DGAT1, FAS, and LPL in adipose tissue: effects of obesity, insulin resistance, and TZD treatment. J Lipid Res. 2006 Nov;47(11):2444-50.

Ren J, Xu N, Zheng H, Tian W, Li H, Li Z, Wang Y, Tian Y, Kang X, Liu X. Expression of Thyroid Hormone Responsive SPOT 14 Gene Is Regulated by Estrogen in Chicken (Gallus gallus). Sci Rep. 2017 Aug 31;7(1):10243.

Rizos CV, Elisaf MS, Liberopoulos EN. Effects of thyroid dysfunction on lipid profile. Open Cardiovasc Med J. 2011 5(76-84.

Roberts CK, Hevener AL, Barnard RJ. Metabolic syndrome and insulin resistance: underlying causes and modification by exercise training. Compr Physiol. 2013 Jan;3(1):1-58.

doi:10.6342/NTU201901578

Rosen ED, Spiegelman BM. Molecular regulation of adipogenesis. Annu Rev Cell Dev Biol. 2000 16(145-71.

Salvado L, Palomer X, Barroso E, Vazquez-Carrera M. Targeting endoplasmic reticulum stress in insulin resistance. Trends Endocrinol Metab. 2015 Aug;26(8):438-48.

Seelig S, Liaw C, Towle HC, Oppenheimer JH. Thyroid hormone attenuates and augments hepatic gene expression at a pretranslational level. Proc Natl Acad Sci U S A. 1981 Aug;78(8):4733-7.

Siersbaek R, Nielsen R, Mandrup S. PPARgamma in adipocyte differentiation and metabolism--novel insights from genome-wide studies. FEBS Lett. 2010 Aug 4;584(15):3242-9.

Silva JE. The thermogenic effect of thyroid hormone and its clinical implications. Ann Intern Med. 2003 Aug 5;139(3):205-13.

Sinha RA, Singh BK, Yen PM. Direct effects of thyroid hormones on hepatic lipid metabolism. Nat Rev Endocrinol. 2018 May;14(5):259-69.

Stelmanska E, Swierczynski J. Up-regulation of lipogenic enzyme genes expression in inguinal white adipose tissue of female rats by progesterone. J Steroid Biochem Mol Biol. 2013 Mar;134(37-44.

Strable MS, Ntambi JM. Genetic control of de novo lipogenesis: role in diet-induced obesity. Crit Rev Biochem Mol Biol. 2010 Jun;45(3):199-214.

Tamura S, Shimomura I. Contribution of adipose tissue and de novo lipogenesis to nonalcoholic fatty liver disease. J Clin Invest. 2005 May;115(5):1139-42.

Tan CE, Ma S, Wai D, Chew SK, Tai ES. Can we apply the National Cholesterol Education Program Adult Treatment Panel definition of the metabolic syndrome to Asians? Diabetes Care. 2004 May;27(5):1182-6.

Thiessen DD, Rodgers DA. Population density and endocrine function. Psychol Bull.

doi:10.6342/NTU201901578

1961 Nov;58(441-51.

Tong Q, Hotamisligil GS. Molecular mechanisms of adipocyte differentiation. Rev Endocr Metab Disord. 2001 Oct;2(4):349-55.

Tseng FY, Chen PL, Chen YT, Chi YC, Shih SR, Wang CY, Chen CL, Yang WS. Association Between Serum Levels of Adipocyte Fatty Acid-binding Protein and Free Thyroxine. Medicine (Baltimore). 2015 Oct;94(41):e1798.

Wallymahmed ME, Baker GA, Humphris G, Dewey M, MacFarlane IA. The development, reliability and validity of a disease specific quality of life model for adults with growth hormone deficiency. Clin Endocrinol (Oxf). 1996 Apr;44(4):403-11.

Wilkin TJ, Voss LD. Metabolic syndrome: maladaptation to a modern world. J R Soc Med. 2004 Nov;97(11):511-20.

Wu J, Wang C, Li S, Li S, Wang W, Li J, Chi Y, Yang H, Kong X, Zhou Y, et al. Thyroid hormone-responsive SPOT 14 homolog promotes hepatic lipogenesis, and its expression is regulated by liver X receptor alpha through a sterol regulatory element-binding protein 1c-dependent mechanism in mice. Hepatology. 2013 Aug;58(2):617-28.

Wu Z, Wang S. Role of kruppel-like transcription factors in adipogenesis. Dev Biol. 2013 Jan 15;373(2):235-43.

Xia X, Serrero G. Inhibition of adipose differentiation by phosphatidylinositol 3-kinase inhibitors. J Cell Physiol. 1999 Jan;178(1):9-16.

Yang WS, Lee WJ, Funahashi T, Tanaka S, Matsuzawa Y, Chao CL, Chen CL, Tai TY, Chuang LM. Weight reduction increases plasma levels of an adipose-derived anti-inflammatory protein, adiponectin. J Clin Endocrinol Metab. 2001 Aug;86(8):3815-9.

doi:10.6342/NTU201901578

Yang WS, Lee WJ, Funahashi T, Tanaka S, Matsuzawa Y, Chao CL, Chen CL, Tai TY, Chuang LM. Plasma adiponectin levels in overweight and obese Asians. Obes Res. 2002 Nov;10(11):1104-10.

Ye J. Mechanisms of insulin resistance in obesity. Front Med. 2013 Mar;7(1):14-24.

Zhang JW, Tang QQ, Vinson C, Lane MD. Dominant-negative C/EBP disrupts mitotic clonal expansion and differentiation of 3T3-L1 preadipocytes. Proc Natl Acad Sci U S A. 2004 Jan 6;101(1):43-7.

Zhang W, Peng W, Zhao M, Lin D, Zeng Z, Zhou W, Bartlam M. Expression, purification and preliminary crystallographic analysis of human thyroid hormone responsive protein. Acta Crystallogr Sect F Struct Biol Cryst Commun. 2011 Aug 1;67(Pt 8):941-6.

Zhu Q, Anderson GW, Mucha GT, Parks EJ, Metkowski JK, Mariash CN. The Spot 14 protein is required for de novo lipid synthesis in the lactating mammary gland. Endocrinology. 2005 Aug;146(8):3343-50.

Zhu Q, Mariash A, Margosian MR, Gopinath S, Fareed MT, Anderson GW, Mariash CN. Spot 14 gene deletion increases hepatic de novo lipogenesis. Endocrinology. 2001 Oct;142(10):4363-70.

doi:10.6342/NTU201901578

Abbreviations

ACC: acetyl-CoA carboxylase

ACLY: ATP-citrate lyase

ADQ: adiponectin

ALT: alanine transaminase

AST: aspartate transaminase

ATP: adenosine triphosphate

BAT: brown adipose tissue

BFP: body fat percentage

BH: body height

BMI: body mass index

BP: blood pressure

BW: body weight

C/EBP: CCAAT/enhaner binding protein

ChIP: chromatin immunoprecipitation

CRE: creatinine

DBP: diastolic blood pressure

DNL: *de novo* lipogenesis

ELISA: enzyme-linked immunosorbent assay

ER: endoplasmic reticulum

FAS: fatty acid synthase

FPG: fasting plasma glucose

fT4: free thyroxine

HbA1c: glycated hemoglobin

doi:10.6342/NTU201901578

HDL-C: high density lipoprotein cholesterol

IFG: impaired fasting glucose

IP-MASS: immunoprecipitation combined with mass spectrometry

KLF: Krüppel-like factor

LDL-C: low density lipoprotein cholesterol

MetS: metabolic syndrome

NAFLD: non-alcoholic fatty liver disease

PPAR: peroxisome proliferator-activated receptor

PPG: postprandial glucose

SBP: systolic blood pressure

SREBP: sterol regulatory element binding protein

T2DM: type 2 diabetes mellitus

T3: triiodothyronine

T4: thyroxine

T-C: total cholesterol

TG: triglyceride

TNF: tumor necrosis factor

THRSP: thyroid hormone responsive protein

TSH: thyroid-stimulating hormone

UA: uric acid

WAT: white adipose tissue

doi:10.6342/NTU201901578

Tables

Table 1. Regulation of S14 in adipocytes or adipose tissue by hormones.

Hormones	Targets	Actions	Species	References
T3				
	3T3-L1 cells	protein, up	mouse	Clement et al., 1987
	White adipose tissue (adipocytes)	mRNA, up	rat	Jump and Oppenheimer, 1985; Freake and Oppenheimer, 1987; Freake and Moon, 2003
	Brown adipose tissue (adipocytes)	mRNA, variable or up	rat	Freake and Oppenheimer, 1987; Perez-Castillo et al., 1993
	3T3-F422A cells	mRNA, no change	mouse	Lepar and Jump, 1989
Hyperthyroid				
	White adipose tissue	mRNA, up	rat	Freake and Oppenheimer, 1987; Blennemann et al,. 1995
	Brown adipose tissue	mRNA, no change	rat	Freake and Oppenheimer, 1987
Dexamethasone				
	3T3-F422A cells	mRNA, up	mouse	Lepar and Jump, 1989
Norepinephrine				
	Brown adipose tissue	mRNA, down	rat	Perez-Castillo et al., 1993
Fasting (low glucose and insulin)				
	White adipose tissue (subcutaneous)	mRNA, down	human	Kirschner and Mariash, 1999
Insulin				
	White and brown adipocytes	mRNA, up	rat	Freake and Moon, 2003
Glucose				
	White and brown adipocytes	mRNA, no change	rat	Freake and Moon, 2003
IGF-1				
	Brown adipose tissue	mRNA, up	rat	Perez-Castillo et al., 1993

IGF-1: insulin-like growth factor 1

doi:10.6342/NTU201901578

Table 2. List of primers and probes used for real-time PCR.

Target name	Forward primer	Reverse primer
36B4	5’-agattcgggatatgctgttggc-3’	5’-tcgggtcctagaccagtgttc-3’
ADQ	5’-accaaaagggctcaggatgc-3’	5’-gtaaagcgaatgggtacatt -3’
S14	5’-cagcctccatcacatcctt-3’	5’-tgtccaggtctcgggtt-3’
S14 probe	5’-gcaggtcctgtaggtctttga-3’	5’-cactcagagggagacggaag-3’
S14R	5’-cgcaagcactgagaacca-3’	5’-ttctccgccctctctaact-3’
pref-1	5’-gaaaggactgccagcacaag-3’	5’-cacagaagttgcctgagaagc-3’
KLF2	5’-accaactgcggcaagacctaca-3’	5’-cgcatcct tcccagttgcaa-3’
KLF3	5’-tacaggagaaaagccgtacaaatg-3’	5’-tcatcagaccgagcgaacttc-3’
KLF4	5’-acagccacccacacttgtgactat-3’	5’ -gtaaggtttctcgcctgtgt -3’
KLF5	5’-acccggatctggagaagcga-3’	5’-cccgtatgagtcctcaggtgagc-3’
KLF6	5’-gagttcctccgtcatttcca-3’	5’-gtcgccattacccttgtcac-3’
KLF7	5’-cacttaaaggcccaccagagg-3’	5’-cactcgcatccttcccatg-3’
KLF9	5’-gtttgcccctgtaagtagtaagtg-3’	5’-ggttcaggccattgtgtagac-3’
KLF15	5’-cgagaagccct t tgcctgca-3’	5’-atcgccggtgccttgacaac-3’
PPARγ2	5’-aagagctgacccaatggttg -3’	5’-gctttatccccacagactcg -3’
C/EBPα	5’-gggtgagttcatggagaatgg-3’	5’-cagtttggcaagaatcagagca-3’
C/EBPβ	5’ -ggggttgttgatgtttttgg-3 ’	5’-cgaaacggaaaaggttctca-3’
C/EBPδ	5’ -ttccaacccctccctgat- 3 ’	5’-ctggagggtttgtgtttttcgt -3’
CHOP10	5’-cggaacctgaggagagagtg-3’	5’- tcataccaggct tccagctc-3’
β-catenin	5’ -gtcagctcgtgtcctgtgaa-3’	5’-cagcttgagtagccattgtcc-3’
SREBP-1	5’-gatcaaagaggagccagtgc-3’	5’-tagatggtggctgctgagtg-3’
GR	5’-gcaagtggaaacctgctatgc-3’	5’-catacatgcagggtagagtcattct-3’
FABP4	5’-gatgaaatcaccgcagacgaca-3’	5’-attgtggtcgactttccatccc-3’
RETN	5’-ccctccttttccttttcttccttg-3’	5’-agactgctgtgccttctggg-3’
ACC1	5’-gagtgactgccgaaacatctctg-3’	5’-gcctcttcctgacaaacgagt-3’
FAS	5’-aggggtcgacctggcctca-3’	5’-tagatggtggctgctgagtg-3’
HSL	5’-gcaagatcaaagcctcagcg-3’	5’-gccaattgtcttctgcgagtgt-3’
LPL	5’-gcccagcaacattatccagt-3’	5’-ggtcagacttcctgctacgc-3’

CHOP: C/EBP homologous protein; FABP: fatty-acid-binding protein;

GR: glucocorticoid receptor; HSL: hormone-sensitive lipase; LPL: lipoprotein lipase;

Pref-1: preadipocyte factor 1; RETN: resistin

doi:10.6342/NTU201901578

Table 3. List of inhibitors used for blocking different signaling pathways.

Inhibitors	Targets	Signaling pathway	Working Concentration	Catalog Number	Company	References
IMD-0354	IKKβ	NFκB	1μM	S2864	Selleckchem	Hino and Nagata, 2012; Kamon et al., 2004
LY294002	PI3K	PI3K	10μM	M1925	Abmole	Smith et al., 1995; Xia and Serrero, 1999
PD98059	MEK1	MAPK	10μM	513000	Calbiochem	Fasshauer et al., 2003; Prusty et al., 2002
SB203580	p38	MAPK	10μM	M1781	Abmole	Engelamn et al., 1998, Engelman et al. 2000
SC-514	IKKβ	NFκB	100μM	3318	TOCRIS	Kishore et al., 2003; Wang et al., 2013
SP600125	JNK	JNK	50μM	S1460	Selleckchem	Chae and Kwak, 2003; Kim et al., 2005
U0126	MEK1	MAPK	10μM	M1977	Abmole	Souza et al., 2003; Tenney et al., 2005

doi:10.6342/NTU201901578

Table 4. Characteristics of subjects with hyperthyroidism or euthyroidism.

	All (male and female)			Male			Female		
	Hyperthyroidism (N=26)	Euthyroidism (N=29)	*P*	Hyperthyroidism (N=9)	Euthyroidism (N=4)	*P*	Hyperthyroidism (N=17)	Euthyroidism (N=21)	*P*
Male:female	9:17	4:25	0.112	9:0	4:0		0:17	0:21	
Age (y)	35.5 (28, 43)	43 (34, 52)	0.028*	39 (27, 43)	38.5 (29, 52)	0.756	34 (29, 39)	44 (35, 52)	0.028*
BH (cm)	162.5 (158, 173)	160 (157, 163)	0.107	174.5 (173, 178)	171 (159, 174.5)	0.188	160 (156, 162)	159 (157, 163)	0.847
BW (kg)	57.5 (53, 61)	58 (55, 67)	0.516	65 (61, 77)	69.5 (55, 73.5)	0.877	56 (50, 58)	58 (55, 64)	0.039*
BMI (kg/m^2)	22.2 (19.5, 23.2)	22.9 (20.9, 26.0)	0.059	20.5 (20.0, 25.3)	22.9 (20.5, 25.1)	0.758	22.3 (19.5, 22.6)	22.9 (20.9, 26.8)	0.050
CRE (mg/dL)	0.6 (0.5, 0.8)	0.7 (0.7, 0.8)	<0.001*	0.8 (0.8, 0.85)	1.0 (0.95, 1.0)	0.007*	0.5 (0.5, 0.6)	0.7 (0.7, 0.8)	<0.001*
AST (U/L)	27 (22, 32)	19 (17, 22)	<0.001*	26 (22, 32)	18.5 (17.5, 22.5)	0.088	27 (24, 31)	19 (16, 22)	<0.001*
ALT (U/L)	36 (29, 49)	14 (12, 18)	<0.001*	33 (32, 41)	14 (13, 22)	0.020*	37 (29, 49)	15 (11, 18)	<0.001*
FPG (mg/dL)	88 (82, 93)	86 (80, 89)	0.190	88 (87, 95)	81 (77, 86)	0.188	88 (82, 93)	87 (84, 89)	0.521
T-C (mg/dL)	143 (120, 170)	200 (182 ,225)	<0.001*	170 (121, 191)	210 (207, 224)	0.006*	137 (120, 158)	191 (182, 225)	<0.001*
TG (mg/dL)	80 (61, 99)	74 (61, 126)	0.607	91 (66,123)	91 (65, 123)	1.000	69 (50, 97)	74 (51, 126)	0.442
HDL-C (mg/dL)	49 (38, 58)	56 (47, 66)	0.041	45 (35, 50)	49 (43, 54)	0.355	53 (41, 59)	58 (47, 66)	0.132
LDL-C (mg/dL)	81 (64, 100)	129 (106, 145)	<0.001*	106 (80, 116)	146 (140, 156)	0.006*	74 (60, 88)	129 (105, 137)	<0.001*
fT4 (ng/dL)	3.36 (2.34, 4.01)	0.98 (0.87, 1.06)	<0.001*	2.34 (2.21, 3.54)	0.93 (0.81, 1.09)	0.006*	3.72 (2.60, 4.01)	0.98 (0.87, 1.06)	<0.001*
TSH (μIU/mL)	0.004 (0.004, 0.006)	1.120 (0.651, 1.630)	<0.001*	0.006 (0.004, 0.013)	1.577 (0.562, 2.755)	0.005*	0.004 (0.004, 0.004)	1.120 (0.665, 1.400)	<0.001*
S14 (ng/mL)	975 (669, 1612)	436 (347, 638)	<0.001*	686 (400, 1683)	717 (437, 1084)	0.877	1037 (731, 1593)	409 (332, 637)	<0.001*
logS14	6.88 (6.51, 7.39)	6.08 (5.85, 6.46)	<0.001*	6.53 (5.99, 7.43)	6.50 (6.08, 6.98)	0.877	6.94 (6.59, 7.37)	6.01 (5.81, 6.46)	<0.001*

Numerical data were presented as median values (Q1, Q3)

Fisher exact test for comparisons of categorical variables between hyperthyroid and euthyroid patients.

Mann-Whitney U tests for comparisons of numerical variables between hyperthyroid and euthyroid patients.

*: $p < 0.05$

doi:10.6342/NTU201901578

Table 5. Univariate regression model with logS14 as dependent variable, and demographic, anthropometric, and laboratory parameters as independent variables.

	All (male and female, N=55)		Male (N=13)		Female (N=42)	
Independent variables	**β (95% CI)**	***P***	**β (95% CI)**	***P***	**β (95% CI)**	***P***
Sex	-0.102 (-0.579, 0.376)	0.671				
Age	-0.017 (-0.035, 0.002)	0.079	0.003 (-0.034, 0.041)	0.846	-0.025 (-0.047, -0.002)	0.033*
BH	0.009 (-0.017, 0.035)	0.472	0.020 (-0.035, 0.075)	0.434	0.003 (-0.049, 0.054)	0.921
BW	-0.007 (-0.027, 0.014)	0.500	0.015 (-0.021, 0.051)	0.385	-0.032 (-0.064, -0.001)	0.042*
BMI	-0.050 (-0.116, 0.016)	0.135	0.034 (-0.093, 0.160)	0.571	-0.088 (-0.168, -0.008)	0.032*
CRE	-1.757 (-2.985, -0.529)	0.006*	-1.308 (-0.5634, 3.018)	0.519	-3.126 (-4.643, -1.609)	<0.001*
AST	0.021 (-0.006, 0.048)	0.123	-0.043 (-0.110, 0.024)	0.184	0.033 (0.003, 0.062)	0.030*
ALT	0.009 (-0.003, 0.021)	0.145	-0.012 (-0.043, 0.018)	0.382	0.013 (-0.0004, 0.026)	0.058
FPG	0.018 (-0.004, 0.041)	0.104	0.040 (-0.008, 0.087)	0.095	0.014 (-0.013, 0.040)	0.300
T-C	-0.006 (-0.010, -0.002)	0.004*	0.002 (-0.010, 0.013)	0.748	-0.008 (-0.012, -0.003)	0.001*
TG	-0.004 (-0.008, -0.001)	0.015*	0.003 (-0.010, 0.016)	0.638	-0.005 (-0.009, -0.001)	0.008*
HDL-C	0.006 (-0.019, 0.007)	0.392	0.015 (-0.021, 0.051)	0.374	-0.008 (-0.024, 0.007)	0.257
LDL-C	-0.007 (-0.013, -0.001)	0.015*	-0.0002 (-0.014, 0.014)	0.970	-0.009 (-0.016, -0.003)	0.007*
fT4	0.213 (0.076, 0.350)	0.003*	0.065 (-0.253, 0.382)	0.663	0.260 (0.101, 0.419)	0.002*
TSH	-0.371 (-0.578, -0.163)	<0.001*	-0.217 (-0.645, 0.211)	0.289	-0.433 (-0.686, -0.180)	0.001*
TSH quartile	-0.302 (-0.457, -0.147)	<0.001*	-0.015 (-0.536, 0.307)	0.562	-0.346 (-0.519, -0.173)	<0.001*

TSH quartile (Group 1: TSH $\leqq$ 0.004; Group 2: 0.004 < TSH $\leqq$ 0.422; Group 3: 0.422 < TSH $\leqq$ 1.17; Group 4: 1.17 < TSH)

*: $p < 0.05$

doi:10.6342/NTU201901578

Table 6. Forward stepwise regression models in all subjects (N=55) with levels of logS14 as dependent variables, and sex, age, anthropometric, and laboratory parameters as independent variables.

Dependent variables	Independent variables	Parameter estimate	Standard error	Model R^2	F	*P*
logS14						
	TSH quartile	-0.3067	0.0799	0.2240	14.72	<0.001*

Forward stepwise regression analysis, variables left in the models are significant at the levels of 0.10.

TSH quartile (Group 1: TSH level ≦ 0.004 μIU/mL; Group 2: 0.004 μIU/mL < TSH level ≦ 0.422 μIU/mL; Group 3: 0.422 μIU/mL < TSH level ≦ 1.17 μIU/mL; Group 4: 1.17 μIU/mL < TSH level)

logS14: log transformation of S14

*: $p < 0.05$

doi:10.6342/NTU201901578

Table 7. Demographic and biochemical characteristics of the subjects with or without metabolic syndrome (MetS).

	With MetS (N = 98)	Without MetS (N = 229)		Total (N = 327)	
Variables	Mean ± SD	Mean ± SD	*p*	Mean ± SD	N
Age (year)	54.2 ± 8.4	52.8 ± 10.2	0.183	53.2 ± 9.7	327
Gender (% male)	75.5%	55.5%	<0.001*	61.5%	
BH (cm)	167.2 ± 8.3	164.1 ± 8.7	0.002*	165.0 ± 8.7	325
BW (kg)	76.3 ± 13.4	62.4 ± 10.6	<0.001*	66.5 ± 13.2	325
BMI (kg/m^2)	26.9 ± 3.2	23.1 ± 2.8	<0.001*	24.2 ± 3.4	324
BFP (%)	29.3 ± 4.1	25.5 ± 5.3	<0.001*	26.7 ± 5.3	324
Waist (cm)	94.6 ± 8.4	83.1 ± 8.1	<0.001*	86.5 ± 9.8	327
Pulse (bpm)	74.3 ± 11.7	71.5 ± 10.8	0.039*	72.4 ± 11.1	327
SBP (mmHg)	129.4 ± 17.0	115.1 ± 12.7	<0.001*	119.4 ± 15.5	327
DBP (mmHg)	79.3 ± 11.9	68.7 ± 9.4	<0.001*	71.9 ± 11.3	327
FPG (mg/dl)	110.6 ± 36.5	93.6 ± 14.0	<0.001*	98.7 ± 24.4	327
PPG (mg/dl)	142.4 ± 63.5	117.3 ± 39.0	<0.001*	124.8 ± 48.9	322
AST (U/L)	22.4 ± 7.9	21.5 ± 8.2	0.341	21.7 ± 8.1	327
ALT (U/L)	26.1 ± 14.4	20.1 ± 10.7	<0.001*	21.9 ± 12.2	327
CRE (mg/dl)	0.9 ± 0.4	0.8 ± 0.2	0.005*	0.9 ± 0.3	327
fT4 (ng/dl)	1.0 ± 0.2	1.1 ± 0.3	0.308	1.1 ± 0.2	327
TSH (μIU/ml)	2.4 ± 1.3	2.2 ± 1.4	0.384	2.3 ± 1.4	327
Hb (g/dl)	15.1 ± 1.4	14.3 ± 1.4	<0.001*	14.5 ± 1.5	327
HbA1c (%)	6.2 ± 1.3	5.6 ± 0.4	<0.001*	5.8 ± 0.8	327
HDL-C (mg/dl)	40.9 ± 9.0	54.3 ± 12.7	<0.001*	50.3 ± 13.2	327
LDL-C (mg/dl)	123.1 ± 30.4	120.8 ± 30.2	0.533	121.5 ± 30.2	327
T-C (mg/dl)	196.7 ± 37.3	194.9 ± 34.2	0.669	195.4 ± 35.1	327
TG (mg/dl)	199.1 ± 136.8	100.7 ± 51.3	<0.001*	130.2 ± 97.2	327
UA (mg/dl)	6.5 ± 1.6	5.7 ± 1.4	<0.001*	6.0 ± 1.5	327
S14 (ng/ml)	87.1 ± 26.3	107.3 ± 40.2	<0.001*	101.2 ±37.7	327

Numerical variables are presented at mean ± standard deviation

*: $p < 0.05$

doi:10.6342/NTU201901578

Table 8. Linear regression analysis with components of metabolic syndrome as independent variables and log transformation of serum S14 level (logS14) as dependent variable, adjusted with age and sex.

	logS14		
Independent variable	**ß**	**95% C.I.**	***p***
Diagnosis of MetS	-0.227	-0.239, -0.088	<0.001*
Central obesity	-0.176	-0.185, -0.048	0.001*
Elevated blood pressure	-0.028	-0.094, 0.056	0.616
Low HDL-C	-0.149	-0.179, -0.032	0.005*
Impaired fasting glucose	-0.035	-0.106, 0.055	0.533
High triglyceride	-0.198	-0.230, -0.069	<0.001*

β: parameter estimate; 95% C.I.: 95% confidence interval. MetS: metabolic syndrome. HDL-C: high density lipoprotein cholesterol

*: $p<0.05$

doi:10.6342/NTU201901578

Table 9. Univariate regression model with components of metabolic syndrome as independent variables and logS14 as dependent variable.

Independent variables	β	95% C.I.	*p*
Age	-0.120	-0.008, 0.000	0.030*
Gender	-0.237	-0.236, -0.086	<0.001*
Central obesity	-0.139	-0.166, -0.018	0.016*
Elevated blood pressure	0.059	-0.038, 0.119	0.307
Low HDL-C	-0.065	-0.126, 0.034	0.259
Impaired fasting glucose	0.000	-0.080, 0.081	0.999
High triglyceride	-0.152	-0.203, -0.027	0.011*

β: parameter estimate; 95% C.I.: 95% confidence interval. HDL-C: high density lipoprotein cholesterol

*: $p<0.05$

doi:10.6342/NTU201901578

Table 10. Odds ratio (95% CI) for MetS and its components according to the quartiles of logS14 with the adjustment of age and gender.

		Odds ratio	95% C.I.
Metabolic syndrome		0.65	0.51, 0.82
	1st quartile	1.00	
	2nd quartile	0.64	0.34, 1.22
	3rd quartile	0.47	0.24, 0.93
	4th quartile	0.25	0.12, 0.54
	P_{trend}: <0.001*		
Central obesity		0.72	0.58, 0.89
	1st quartile	1.00	
	2nd quartile	0.77	0.41, 1.44
	3rd quartile	0.65	0.34, 1.24
	4th quartile	0.35	0.18, 0.68
	P_{trend}: 0.002*		
Elevated blood pressure		0.94	0.75, 1.16
	1st quartile	1.00	
	2nd quartile	0.74	0.39, 1.42
	3rd quartile	0.95	0.49, 1.84
	4th quartile	0.74	0.38, 1.47
	P_{trend}: 0.551		
Low HDL-C		0.76	0.61, 0.95
	1st quartile	1.00	
	2nd quartile	1.01	0.53, 1.91
	3rd quartile	0.82	0.42, 1.58
	4th quartile	0.41	0.20, 0.84
	P_{trend}: 0.015*		
Impaired fasting glucose		0.96	0.76, 1.22
	1st quartile	1.00	
	2nd quartile	0.76	0.38, 1.52
	3rd quartile	0.68	0.33, 1.40
	4th quartile	0.93	0.45, 1.92
	P_{trend}: 0.745		
High triglyceride		0.65	0.51, 0.83
	1st quartile	1.00	
	2nd quartile	0.85	0.44, 1.65
	3rd quartile	0.55	0.27, 1.14
	4th quartile	0.24	0.10, 0.57
	P_{trend}: 0.001*		

HDL-C: high density lipoprotein cholesterol, MetS: metabolic syndrome

*: $p < 0.05$

doi:10.6342/NTU201901578

Table 11. List of the regulated genes by IL-1β treatment in 3T3-1 adipocytes.

Rank	UniGene ID	Gene Symbol	Chip fold change	Real-Time PCR confirmed fold change
Up-regulation				
1	Mm.284248	Ccl5	110.35	132.6
2	Mm.3485	Hpx	62.63	26.9
6	Mm.9537	Lcn2	21.00	1220.1
7	Mm.218846	Lbp	19.08	111.9
13	Mm.228363	Oasl2	12.47	8.4
17	Mm.26730	Hp	12.08	16.9
36	Mm.4791	Ereg	6.83	9.7
37	Mm.371583	Slpi	6.77	30.9
Down-regulation				
1	Mm.28585	S14	7.37	12.5

Only list the genes have been studied

doi:10.6342/NTU201901578

Table 12. IP-MASS data: Protein ID in mS14-flag but not in vector.

up1	up2	up3	up4	up5	bottom
NRBP2	HV305	---	PIP	K2C6A	ZA2G
	IGHG1		K2C74	ZA2G	S10A8
	UNC79		SHRM3	K1C17	ACTB
			E2AK4	CATD	LYSC
			APOD	APOD	DHSD
			S12A3	G3P	UNC79
			TRI56	**THRSP**	APOD
				ANXA2	DCD
				IGHG1	K2C71
				IGKC	KLF7
				H3C	
				BROMI	
				ARRC	
				DYH14	
				IDUA	
				DYST	
				MARH7	
				POK5	
				SYN2	

doi:10.6342/NTU201901578

Figures

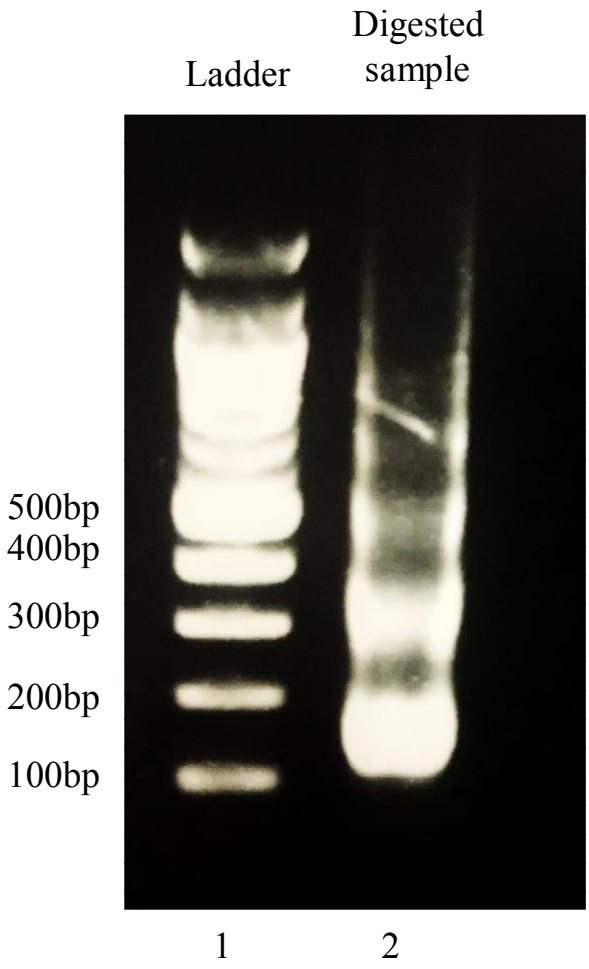

Figure 1. The pattern of digested DNA sample. 3T3-L1 cells were formaldehyde-crosslinked and chromatin was prepared and digested as described in material and methods. DNA was purified as described and 10 μl were separated by electrophoresis on a 1% agarose gel (lane 2) and stained with ethidium bromide.

doi:10.6342/NTU201901578

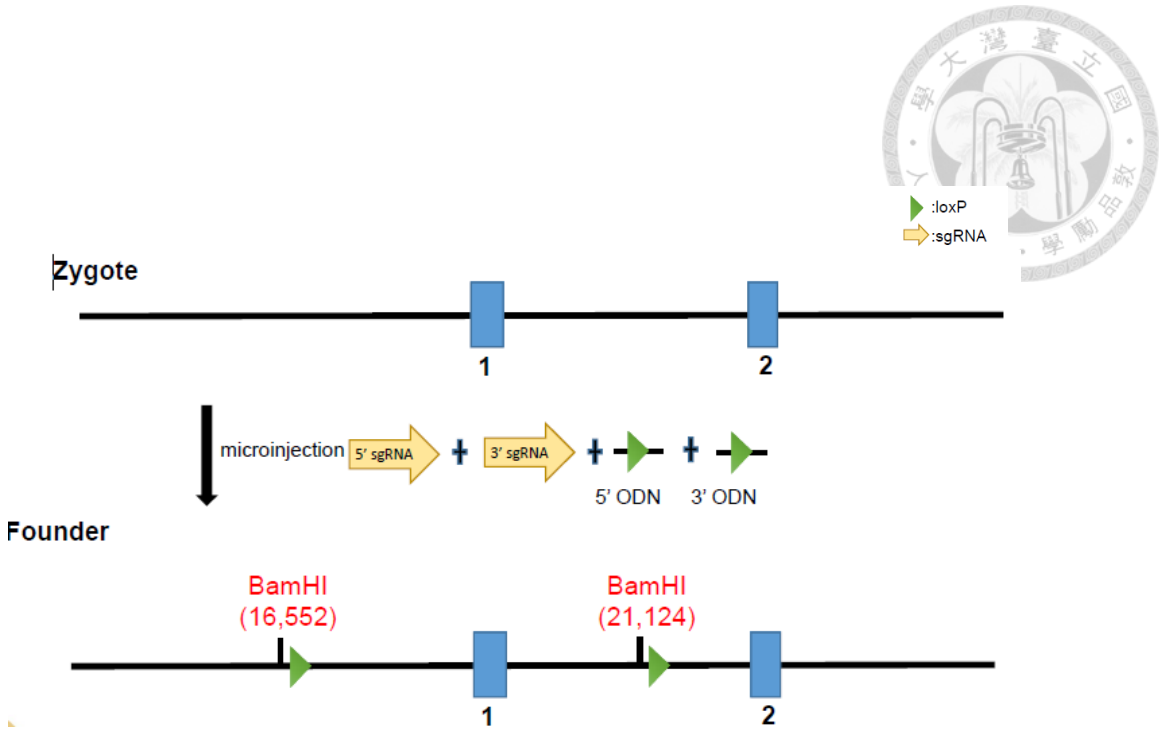

Figure 2. The strategy design of *S14* conditional knockout mice. To create conditional *S14* exon 1 deletion mice, mouse ES cells were transfected with target specific sgRNAs and *loxp* oligodeoxynucleotides (ODN) with BamHI restriction enzyme cutting sites.

doi:10.6342/NTU201901578

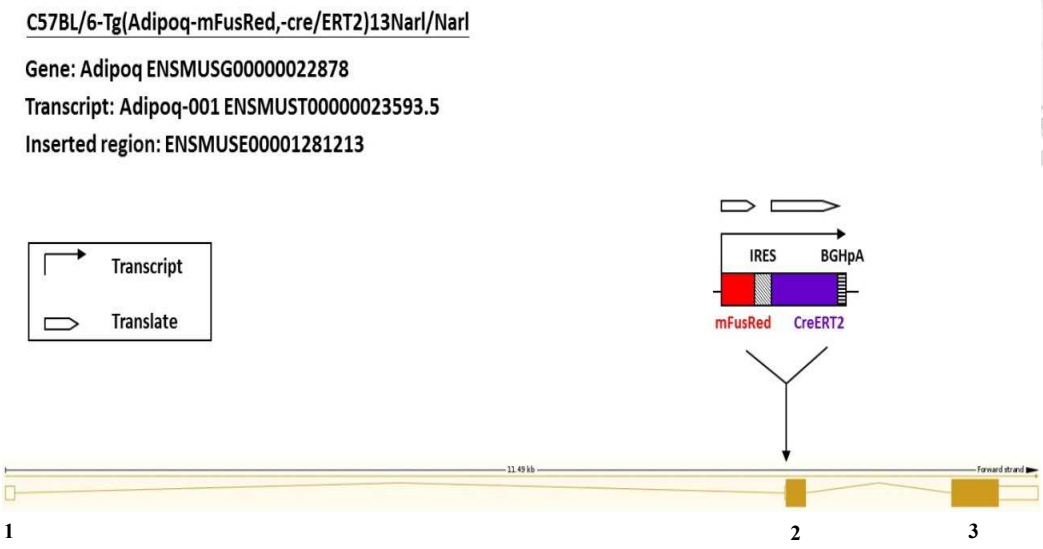

Figure 3. The gene background information of C57BL/6-Tg(Adipoq-FusRed, -cre/ERT2)13Narl mice from Rodent Model Resource of National Laboratory Animal Center. The CreERT2 cassette containing internal ribosome entry site (IRES) and membrane-associated FusRed was inserted in the exon 2 of *Adipoq* gene.

doi:10.6342/NTU201901578

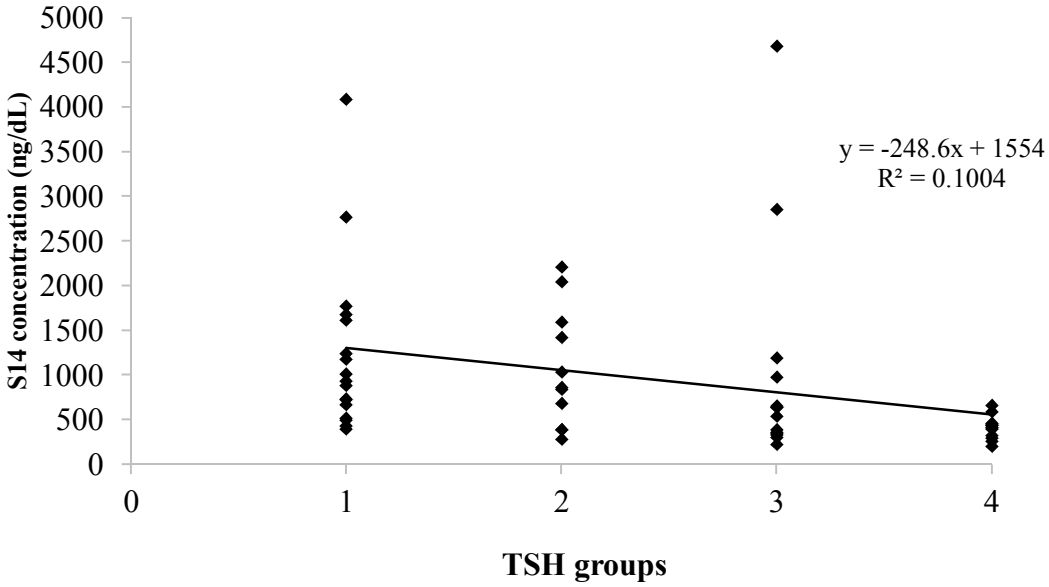

Figure 4. A negative relationship between logS14 and TSH levels in which the subjects were divided into 4 groups based on their TSH levels. TSH quartile (Group 1: TSH level ≦ 0.004 μIU/mL; Group 2: 0.004 μIU/mL < TSH level ≦ 0.422 μIU/mL; Group 3: 0.422 μIU/mL < TSH level ≦ 1.17 μIU/mL; Group 4: 1.17 μIU/mL < TSH level) (Chen et al., 2016)

doi:10.6342/NTU201901578

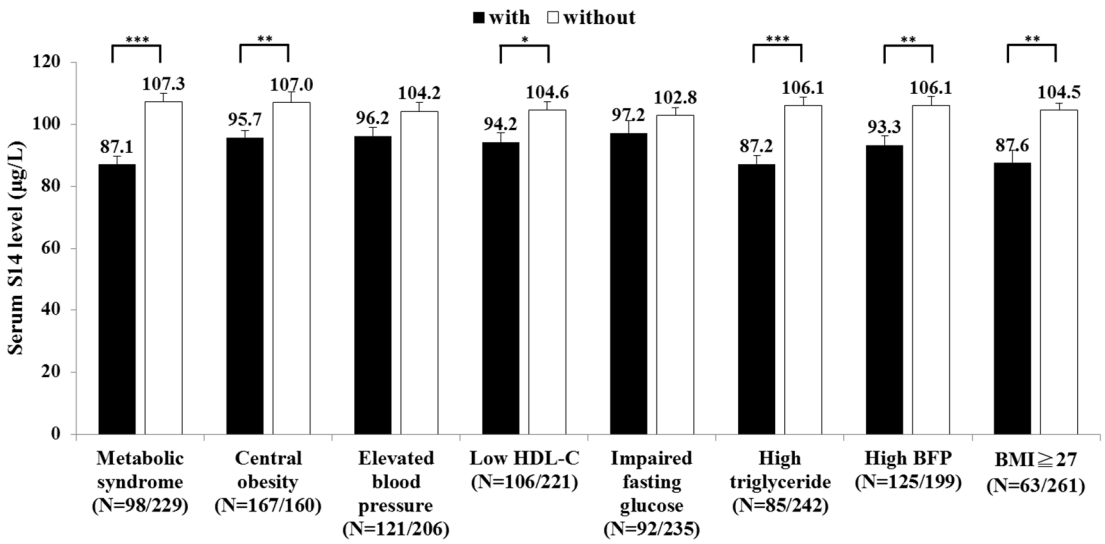

Figure 5. Comparison of serum S14 levels between the subjects with and without MetS or related components. The S14 levels of the subjects with and without the components were respectively shown with black and white bars. The cut-off points of BFP for men were 25.0% and for women were 35.0%. The data were shown as mean and standard error. N shows the individual number. * $p<0.05$, ** $p<0.01$, *** $p<0.001$. (Chen et al., 2019)

doi:10.6342/NTU201901578

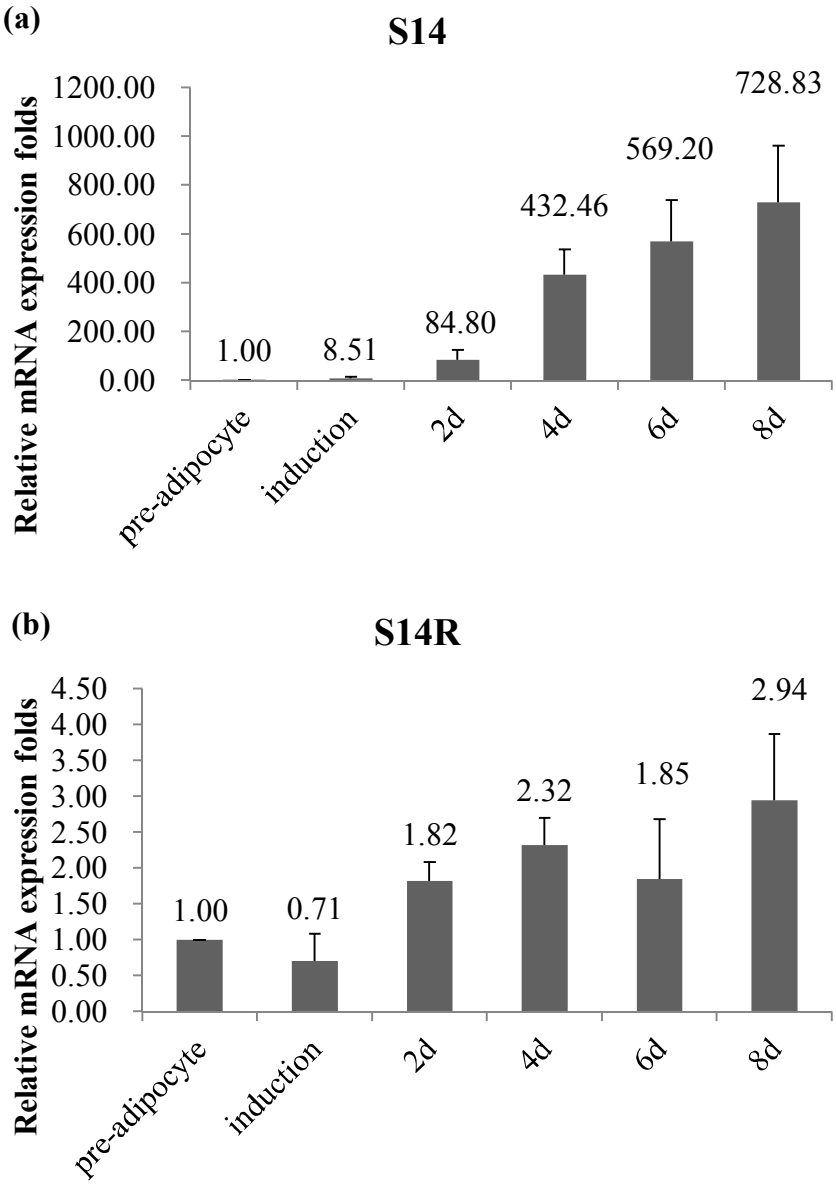

Figure 6. The mRNA levels of S14 and S14R increased during 3T3-L1 adipocyte differentiation. The relative mRNA expression levels of (a) S14 and (b) S14R during 3T3-L1 adipocytes differentiation analyzed by real-time qPCR were shown. The gene expression levels of pre-adipocytes were set as 1.0. The error bars referred to the standard deviation obtained in three or more independent experiments.

doi:10.6342/NTU201901578

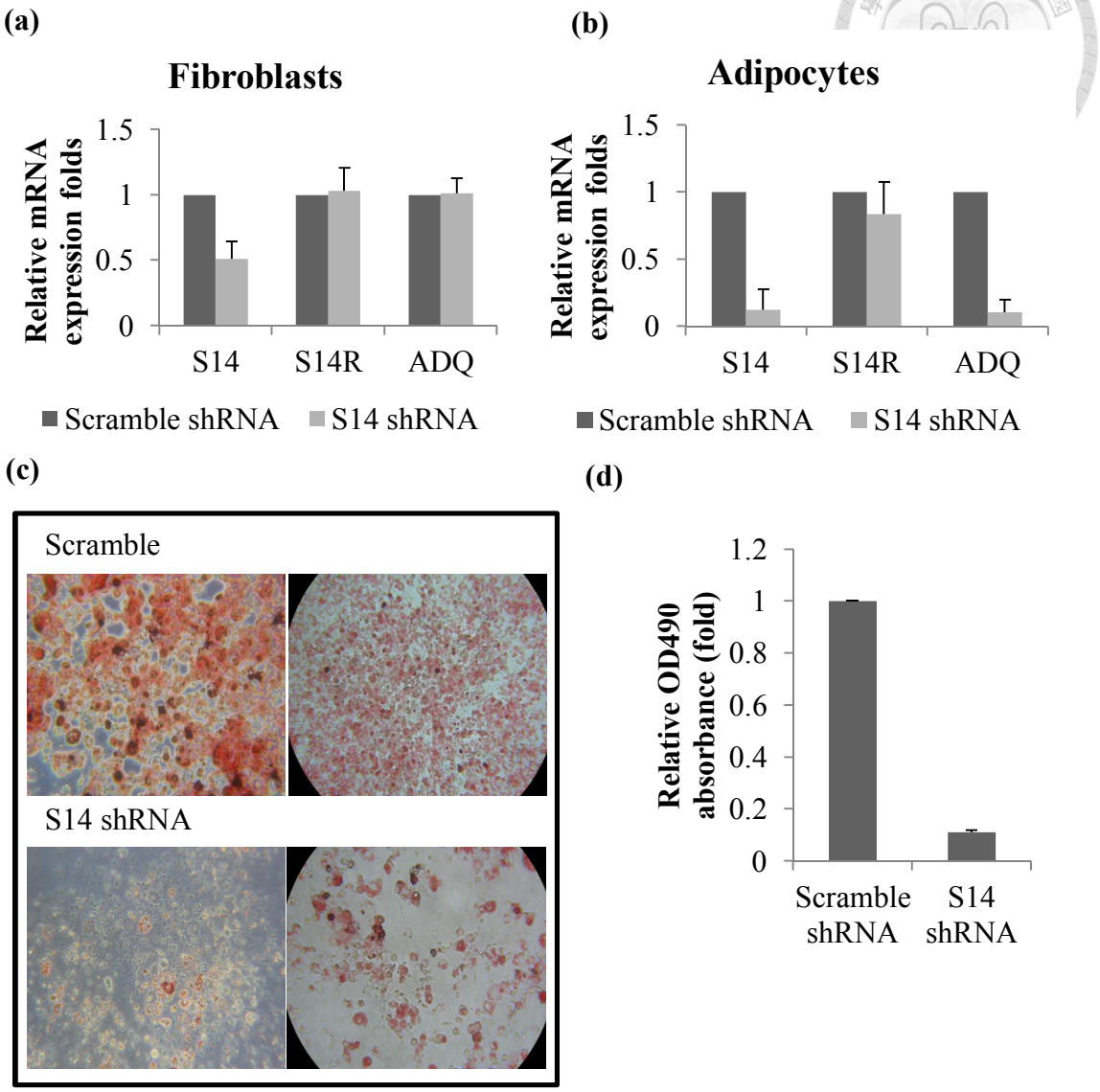

Figure 7. Knockdown of S14 repressed 3T3-L1 lipid droplets accumulation. After lentiviral transduction, the relative mRNA expression levels compared to the control in (a) 3T3-L1 fibroblast and in (b) differentiated 3T3-L1 adipocyte were shown. (c) The lipid accumulations of S14 knockdown and control cells were stained with oil red O. (d) Oil red O was extracted using isopropanol, and OD_{490} was measured to quantify triglyceride accumulation. The error bars referred to the standard deviation obtained in three or more independent experiments.

doi:10.6342/NTU201901578

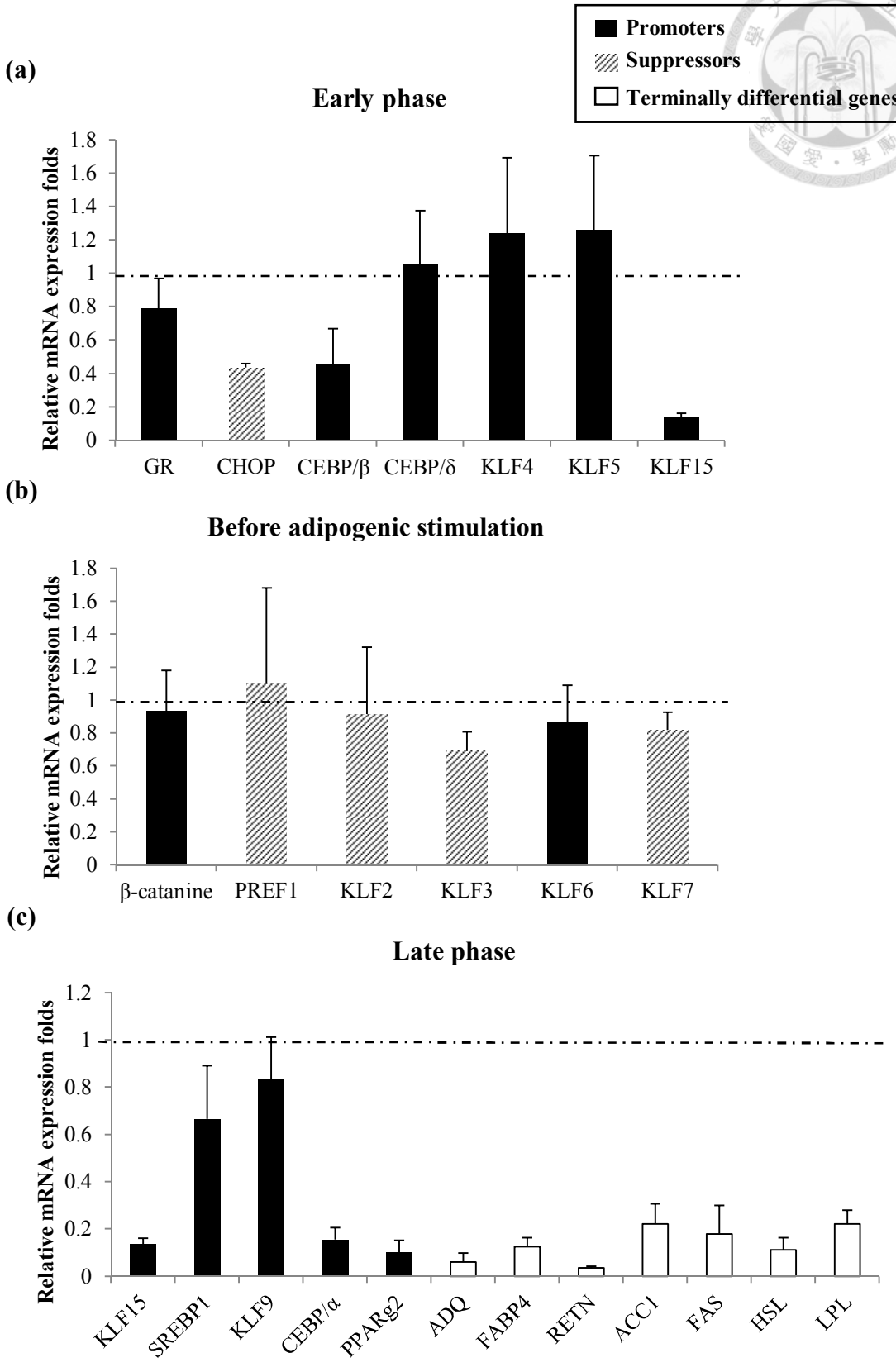

Figure 8. S14 knockdown altered differentiation-related gene expression during 3T3-L1 adipocyte differentiation. After knocking down S14 in 3T3-L1 pre-adipocyte,

doi:10.6342/NTU201901578

the mRNA expression levels of differentiation-related genes were analyzed by real-time qPCR compared to the control cells. The differentiation process is arbitrarily divided into three stages: (a) before adipogenic stimulation, (b) early phase and (c) late phase. The error bars referred to the standard deviation obtained in three or more independent experiments.

doi:10.6342/NTU201901578

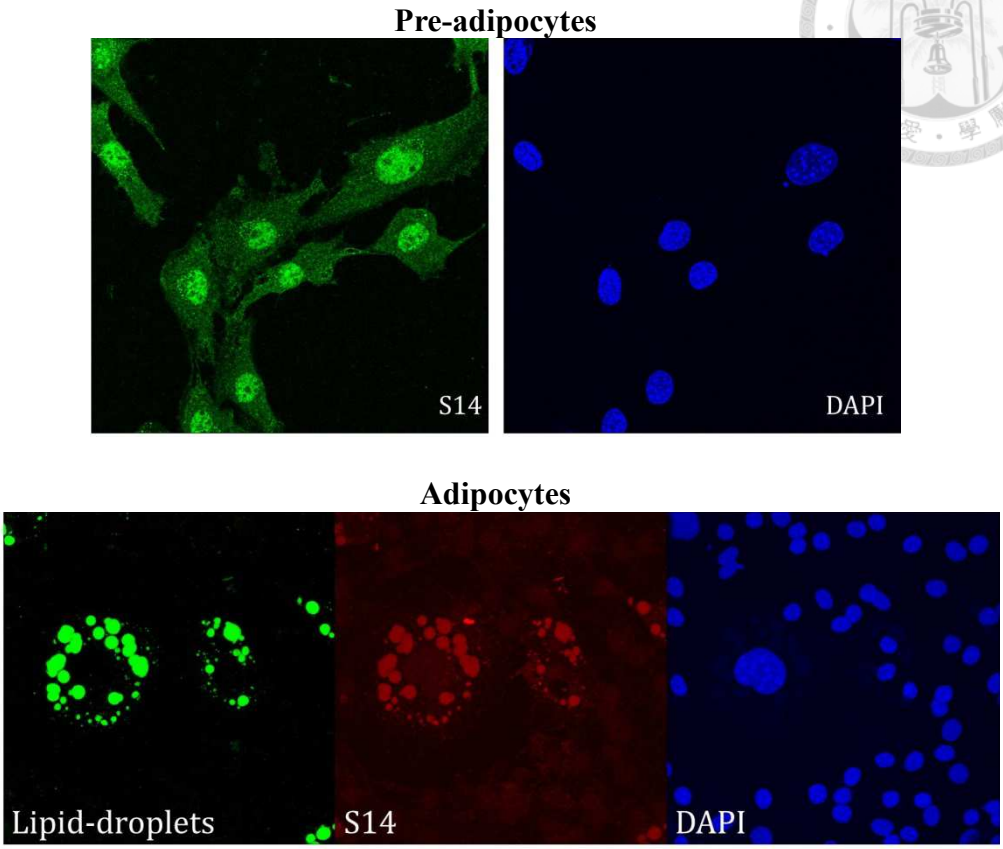

Figure 9. The locations of S14 in 3T3 L1 fibroblast and adipocyte by immunofluorescence. Mouse 3T3-L1 pre-adipocytes and adipocytes stained with and anti-S14 rabbit polyclonal antibody. The images were captured in the three different channels for Alexa Fluor 594 (pseudo-colored red, S14), Alexa Fluor 488 (pseudo-colored green, S14), BODIPY 493/503 (pseudo-colored green, lipid droplets) and DAPI (pseudo-colored blue, nuclei-DNA) on a Leica TCS SP5 confocal microscopy system with a 20x objective.

doi:10.6342/NTU201901578

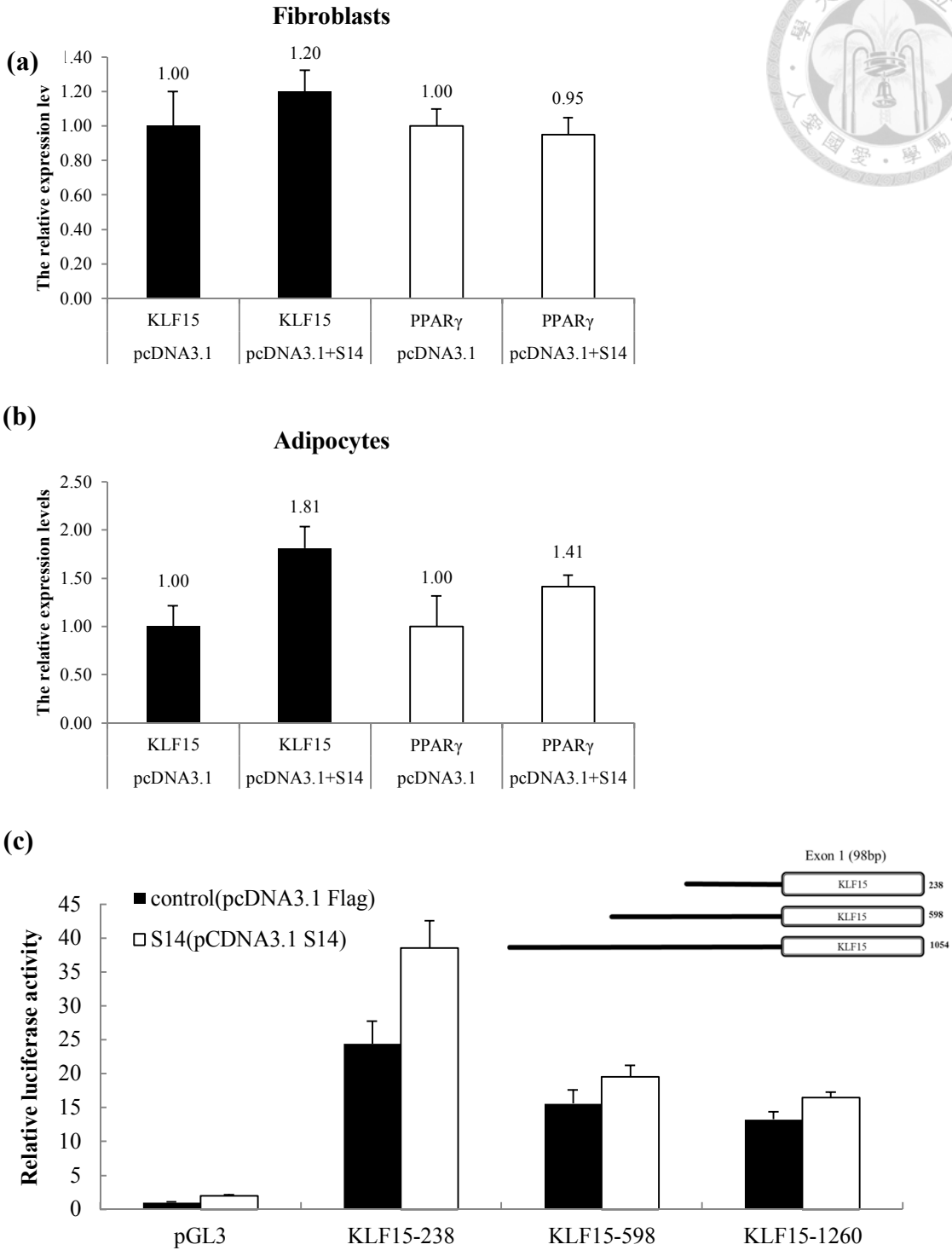

Figure 10. Effects of S14 overexpression on KLF15 and PPARγ promoter activities in undifferentiated and differentiated 3T3-L1 cells. Relative luciferase activity expression levels of co-transfection S14-overexpressed construct and KLF15 or PPARγ2 promoters in (a) 3T3-L1 fibroblasts and (b) adipocytes. (c) Relative luciferase

doi:10.6342/NTU201901578

activity expression levels of co-transfection S14-overexpressed construct and promoter deletion constructs of KLF15 in 3T3-L1 pre-adipocytes.

doi:10.6342/NTU201901578

(a)

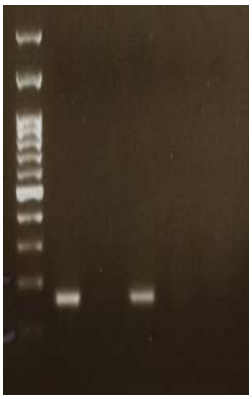

Primer	Sample No.	IP condition
mouse RPL30	1	Histone positive
	2	Rabbit IgG negative
	3	2%input
	4	without Antibody negative control
	5	without DNA negative control
Anneal : 62℃		
Reagent: Thermo dream Taq 2X master Mix		
cycles: 29		

(b)

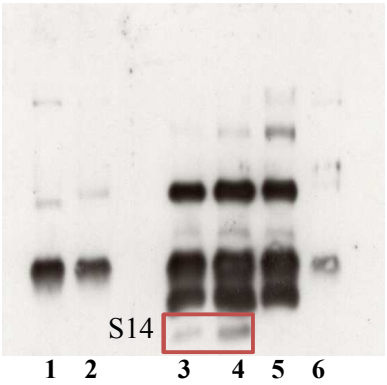

Sample No.	IP condition
1	Histone positive
2	Rabbit IgG negative
3	Anti-S14 5ug
4	Anti-S14 10ug
5	Goat IgG negative control
6	2% input

Figure 11. Process confirmation of ChIP assay. (a) Purified DNA was analyzed by standard PCR methods using Human RPL30 Exon 3 primers. PCR products were observed for histone positive ChIP sample (lane 1) and imput sample (lane 3) but not in the normal rabbit IgG or other negative control ChIP samples (lane 2, 4, 5). (b) S14 protein existed in the chromatin sample sections (lane 3 and 4) but not in other control samples by Western blot.

doi:10.6342/NTU201901578

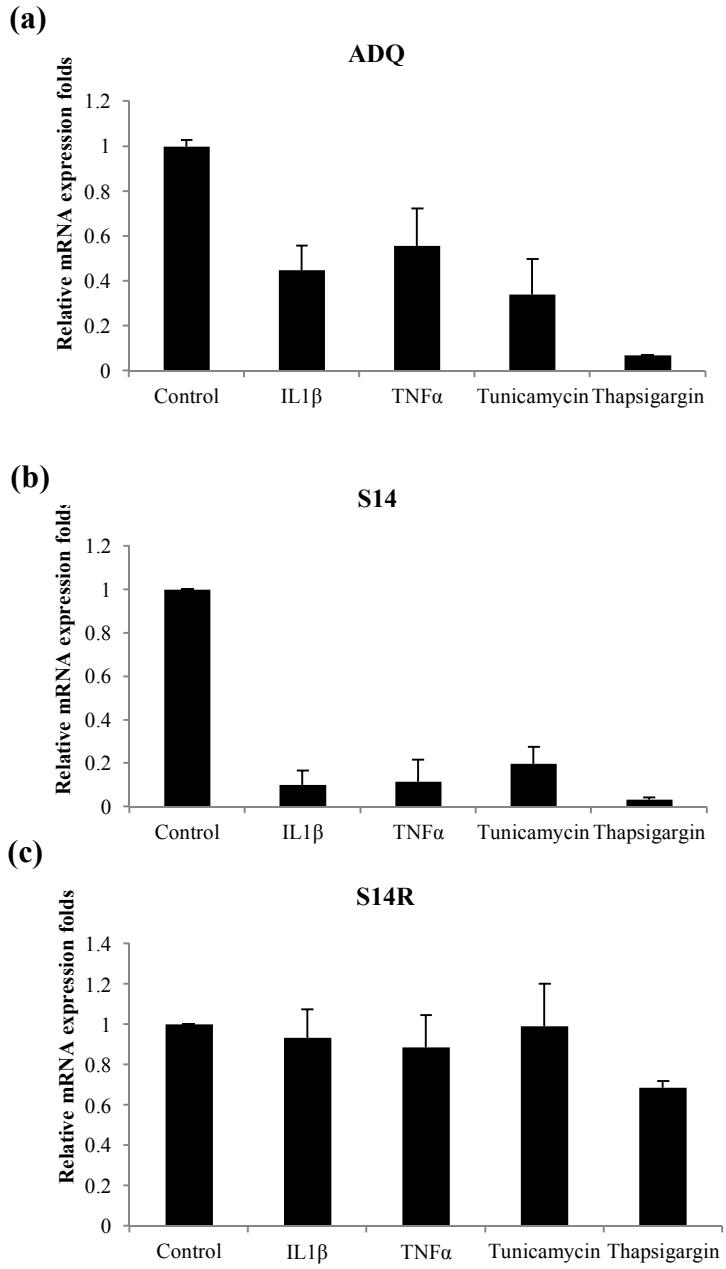

Figure 12. The S14 mRNA was reduced with the treatment of cytokines and ER stress inducers. The relative mRNA expression levels of (a) adiponectin, (b) S14 or (c) S14R with different treatments as indicated in adipocytes were shown. The error bars referred to the standard deviation obtained in three or more independent experiments.

doi:10.6342/NTU201901578

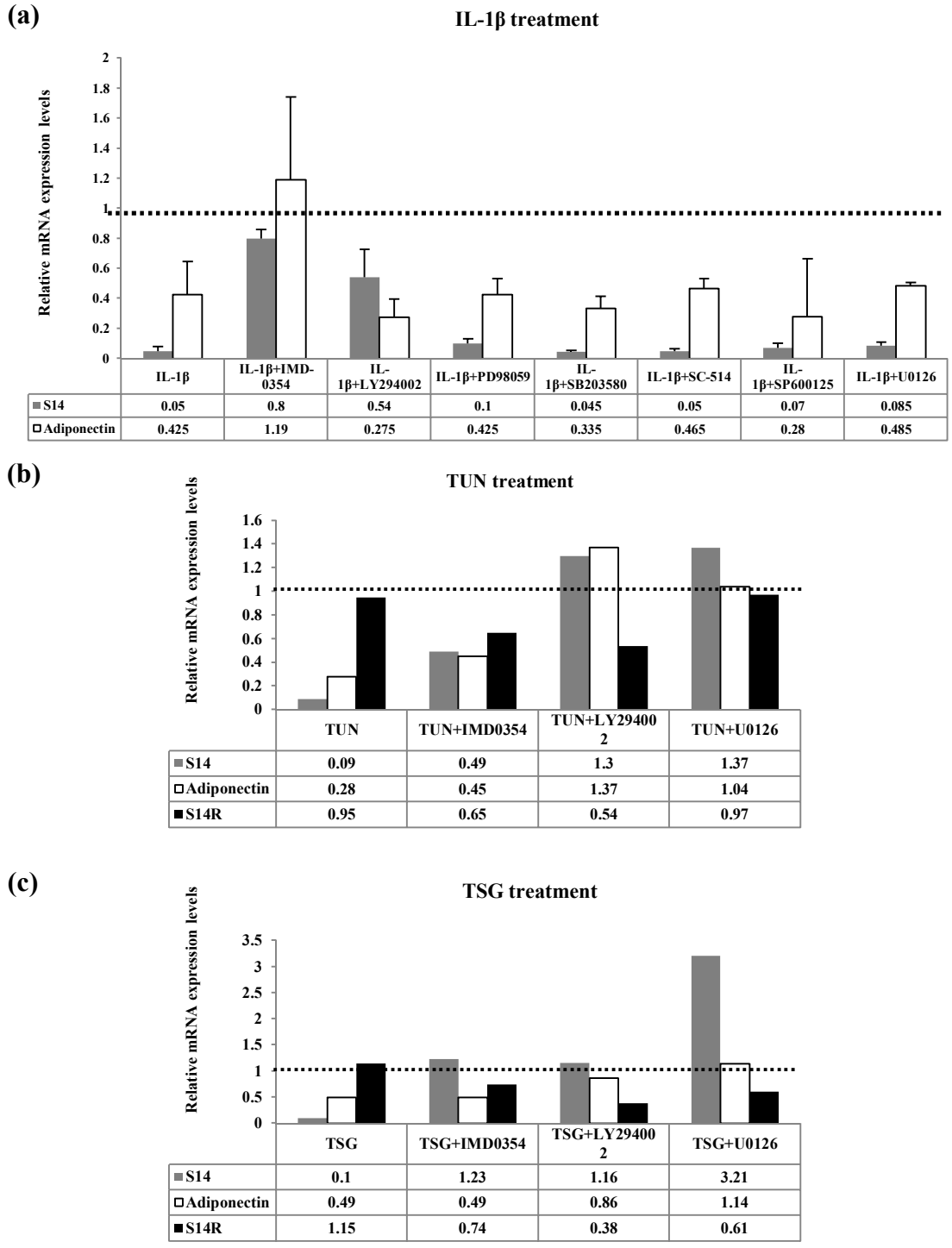

Figure 13. The IL-1β- or ER stress inducers-mediated S14 mRNA downregulation was recovered with the NF-κB, PI3k or ERK signaling inhibitors treatment. The relative mRNA expression levels of S14, adiponectin, and S14R with (a) IL-1β (b)

doi:10.6342/NTU201901578

Tunicamycin (TUN) and (c) thapsigargin (TSG) with different inhibitors treatment in adipocytes were shown.

doi:10.6342/NTU201901578

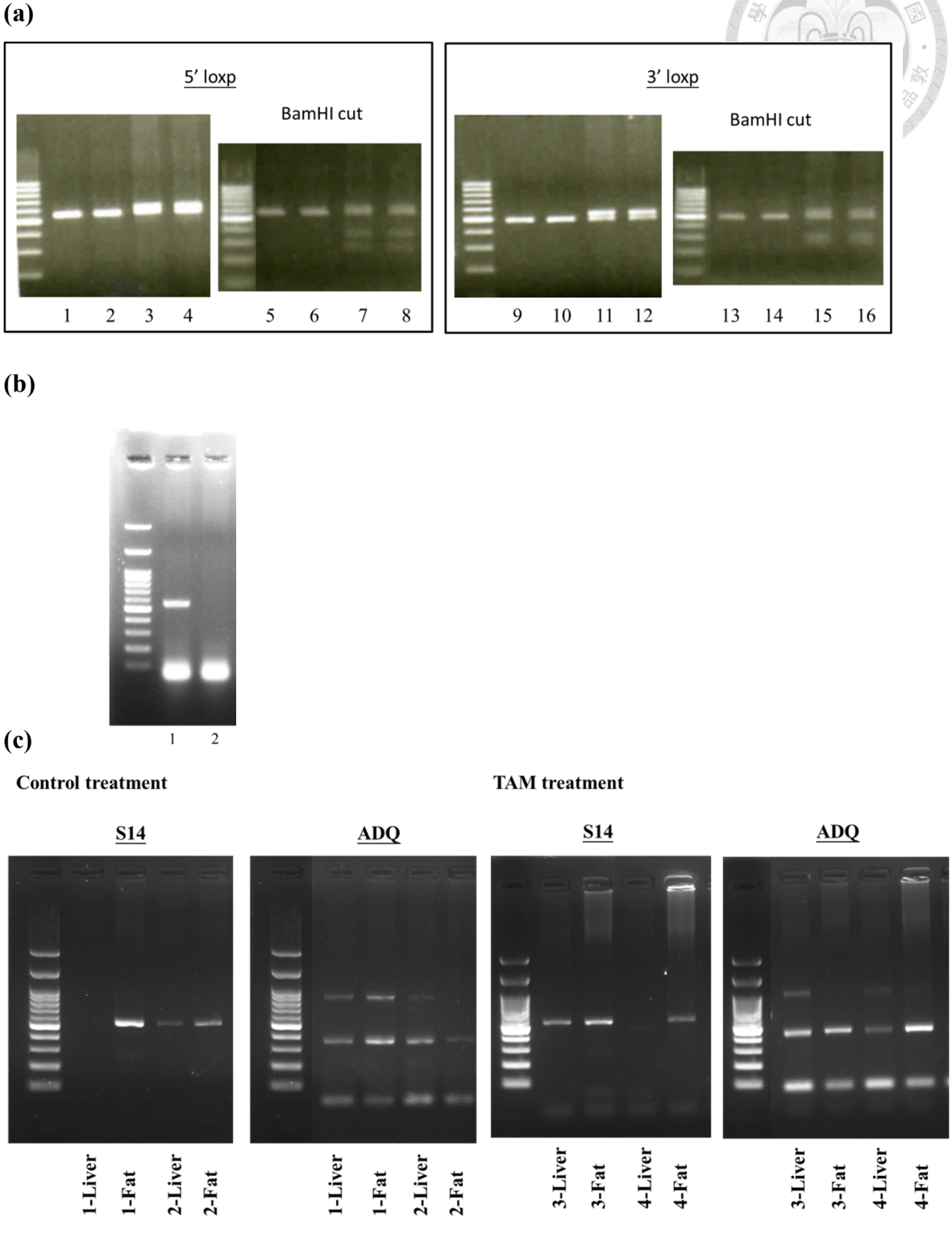

Figure 14. PCR genotyping for adipose tissue-specific conditional S14 knockout mice. (a) 5', 3' primers and BamHI restriction enzyme were used to check the DNA rearrangement patterns of C57BL/6J-*Thrsp*-loxp strain mice. Wild type: lane 1, 2, 5, 6,

doi:10.6342/NTU201901578

9, 10, 13,14; *Thrsp*-loxp inserted: lane 3, 4, 7, 8, 11, 12, 15, 16. (b) CreF and CreR primers were used to check the DNA rearrangement patterns of C57BL/6-*Adipoq*-cre mice. Lane 1: mouse with *adipoq*-cre; lane 2: mouse without *adipoq*-cre. (c) The DNA rearrangement patterns of S14 in mice liver and adipose tissue with intraperitoneal injection of tamoxifen (TAM) or not.

doi:10.6342/NTU201901578

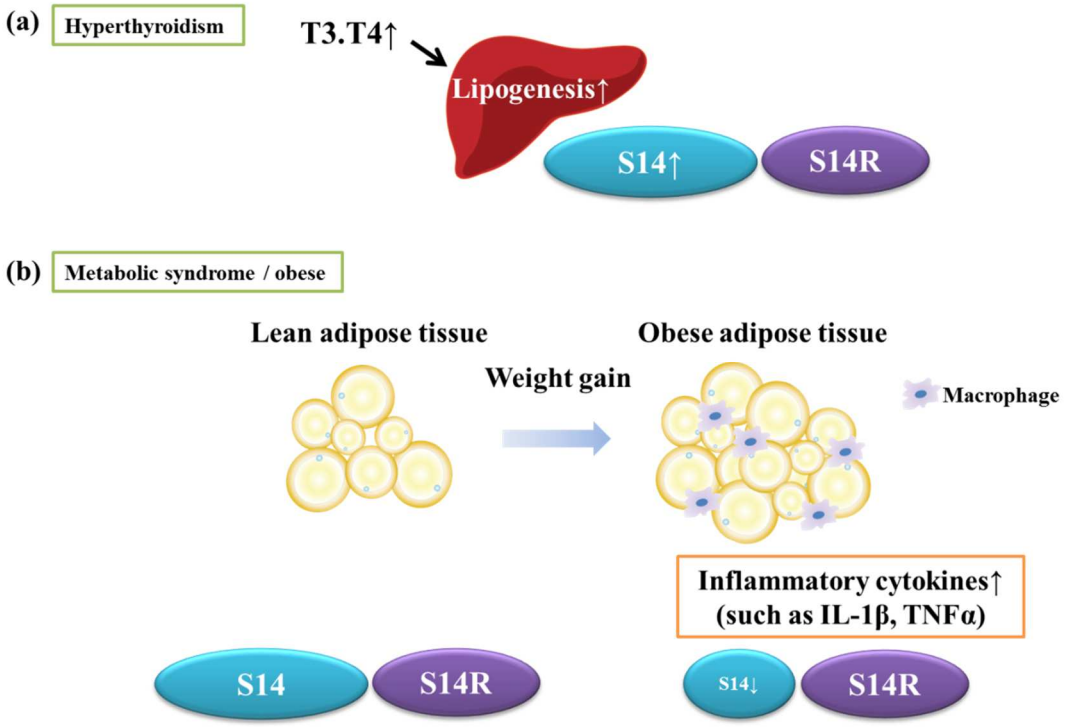

Figure 15. Models of S14 in endocrine and metabolic disorders. (a) In hyperthyroidism, thyroid hormones induce hepatic *de novo* lipogenesis. Liver might be the main sources of the increased serum S14. (b) In metabolic syndrome or obese status, inflammatory cytokines are increased around the adipose tissue might down-regulated serum S14 expression.

doi:10.6342/NTU201901578

Publications related to this thesis

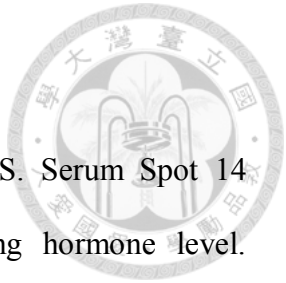

1. **Chen YT**, Tseng FY, Chen PL, Chi YC, Han DS, Yang WS. Serum Spot 14 concentration is negatively associated with thyroid-stimulating hormone level. Medicine (Baltimore) 2016 Oct;95(40):e5036
2. **Chen YT**, Tseng PH, Tseng FY, Chi YC, Han DS, Yang WS. The serum level of a novel lipogenic protein Spot 14 was reduced in metabolic syndrome. PLoS One 2019 Feb 14;14(2):e0212341

doi:10.6342/NTU201901578